Final Report Submitted to
the National Aeronautics and Space Administration
Planetary Atmospheres Program
for Grant NASW-1946
Entitled:

The Kinetics and Dynamics of the Coma of Halley's Comet

by Michael R. Combi

Space Physics Research Laboratory
Department of Atmospheric, Oceanic and Space Sciences
University of Michigan
Ann Arbor, MI 48109

January 1994

I. Introduction

This grant to the University of Michigan supported the efforts of Michael R. Combi to serve as a Co-Investigator in collaboration with a larger effort by the Principal Investigator, William Smyth of Atmospheric and Environmental Research, Inc. The overall objective of this project was to analyze in a self-consistent manner unique optical $O(^1D)$ and NH_2 ultra-high resolution line profile data of excellent quality and other supporting lower-resolution spectral data for the coma of comet P/Halley by using highly developed and physically-based cometary coma models in order to determine and explain in terms of physical processes the actual dynamics and photochemical kinetics that occur in the coma. The justification for this work is that it provides a valuable and underlying physical base from which to interpret significantly different types of coma observations in a self-consistent manner and hence bring into agreement (or avoid) apparent inconsistencies that arise from non-physically based interpretations. The level of effort for the Michigan component amounted to less than 3 person-months over a planned period of three years. The period had been extended at no extra cost to four years because the Michigan grant and the AER contract did not have coincident time periods. An effort of somewhat larger scope was undertaken by the PI.

The importance of the $O(^1D)$ profiles is that they provide a direct trace of the water distribution in comets. The line profile shape is produced by the convolution of the outflow velocity and thermal dispersion of the parent water molecules with the photokinetic ejection of the oxygen atoms upon photodissociation of the parent water molecules. Our understanding of the NH_2 and its precursor ammonia are important for comet-to-comet composition variations as they relate to the cosmo-chemistry of the early solar nebula. Modeling of the distribution of NH_2 is necessary in order to infer the ammonia production rates from NH_2 observations.

II. Accomplishments for the University of Michigan Effort

This project represented a very well-focused effort to analyze interferometric spectra of comet P/Halley, obtained by Fred Roesler, Frank Scherb and student co-workers at the University of Wisconsin during 1985 and 1986. Since the technical details and scientific results are presented in great detail in the accompanying paper (Smyth et al. 1994) only a brief summary of the work and the results will be given specifically as part of the main body of this report. This paper has already been submitted for publication in The Astrophysical Journal.

The portion of the work done at the University of Michigan involved the actual modeling analysis of the line profiles of O(^{1}D) and NH_2 provided by the Wisconsin group and participation with the PI and the Wisconsin group in the interpretation of the data. A slight variation of our coma models (Combi and Smyth 1988 a&b; Combi 1989), which had been to analyze similar but already published data, including radio line profiles, was used for the analysis of the Wisconsin interferometric data.

The principal results were as follows:

1. The Monte Carlo Particle Trajectory Model provided excellent agreement with both O(^{1}D) and NH_2 line profiles from 1986 data obtained in January (r=0.78AU) and May (r=1.67AU). This verifies the underlying dynamics, exothermic photodissociative chemisty, and collisional thermalization in the coma.

2. The somewhat wider O(^{1}D) line profile in January compared with May confirms the variation of the coma outflow speed with heliocentric distance.

3. The narrow January NH_2 line profile is indicative of the outflow dynamics of the parent molecules in the coma because of the very short photodissociation time of the NH_2 parent (presumable NH_3) and as such is consistent with the dynamics implied by the O(^{1}D) line profile and other data.

4. The average water production rates derived from the O(^{1}D) line profiles were 2.90 and 2.68 x 10^{30} molecules per second for January 16 and 17, respectively. They were found to be consistent with the extrapolated water production rates determined by the previously published low resolution observations of O(^{1}D) and Hα (Smyth et al. 1993) and the 7.6-day photometric light curve of Schleicher et a. (1990). These large values establish that the maximum water production rate for comet Halley actually occurred during the 2-3 weeks prior to perihelion. Implications drawn from the collisionally quenched OH 18-cm radio observations in later January indicate that the water production rate may have been as large as 3.6 x 10^{30} molecules per second near January 23, but this is more speculative.

5. The NH_3 production rate determined from the NH_2 line profile of January 17 was 1.48 x 10^{28} per second, yielding an NH_3/H_2O production rate ratio of 0.55%, which is consistent with most other measures from NH_2 and NH observations when analyzed with improved and consistent g-factors for NH_2.

6. Perhaps most importantly, the MCPTM in combination with the hybrid dusty-gas dynamic/Monte Carlo model have now been successful in analyzing and explaining a wide variety of observations of the water dissociation products in comet Halley, including line widths of published radio OH profiles (Combi 1989), wide field Lyman-α images and scans (Smyth, Combi and Stewart 1991; Smyth et al. 1994), IUE Lyman-α

observations (Combi and Feldman 1993), IUE OH observations (Combi, Bos and Smyth 1993), and O(^{1}D) and Hα observations (Smyth et al. 1993). These results now present reasonably self-consistent analyses of water production rates and water dissociation product kinetics and dynamics.

References

Combi, M.R. 1989. The outflow speed of the coma of Halley's comet. *Icarus* **81**, 41-50.

Combi, M.R., B.J. Bos and W.H. Smyth. 1993. The OH distribution in cometary atmospheres: A collisional Monte Carlo model for heavy species. *Astrophys. J.* **408**, 668-677.

Combi, M.R. and P.D. Feldman. 1993. Water production rates in comet P/Halley from IUE observations of HI Lyman-α. *Icarus* **105**, 557-567.

Combi, M.R. and W.H. Smyth. 1988a. Monte Carlo particle trajectory models for neutral cometary gases. I. Models and equations. *Astrophys. J.* **327**, 1026-1043.

Combi, M.R. and W.H. Smyth. 1988b. Monte Carlo particle trajectory models for neutral cometary gases. II. The spatial morphology of the Lyman-alpha coma. *Astrophys. J.* **327**, 1044-1059.

Schleicher, D.G., R.L. Millis, D.T. Thompson, P.V. Birch, R.M. Martin, D.J. Tholen, J.R. Piscitelli, N.L. Lark, and H.B. Hammel. 1990. Periodic variations in the activity of comet P/Halley during the 1985/1986 apparition. *Astron. J.* **100**, 896-912.

Smyth, W.H., M.R. Combi and A.I.F Stewart. 1991. Analysis of the Pioneer Venus Lyman-α Image of the Hydrogen Coma of Comet P/Halley. *Science* **253**, 1008-1010.

Smyth, W.H., M.L. Marconi, and M.R. Combi. 1994. Analysis of hydrogen Lyman-a observations of the coma of comet P/Halley near perihelion. *Icarus* (submitted).

Smyth, W.H., M.L. Marconi, F. Scherb, and F.L. Roesler. 1993. Analysis of hydrogen Ha observations of the coma of comet P/Halley. *Astrophys J.* **413**, 756-763.

APPENDIX

"Observations and Analysis of O(1D) and NH2 Line Profiles for the Coma of Comet P/Halley"

by W.H. Smyth, M.R. Combi, F.L Roesler and F. Scherb

Submitted to
The Astrophysical Journal
October 1993

Observations and Analysis of $O(^1D)$ and NH_2 Line Profiles for the Coma of Comet P/Halley

William H. Smyth[1]

Michael R. Combi[2]

Fred L. Roesler[3,4]

Frank Scherb[3,4]

Submitted to

The Astrophysical Journal

October 6, 1993

1. Atmospheric and Environmental Research, Inc., 840 Memorial Drive, Cambridge, MA 02139 (Mailing address)
2. Space Physics Research Laboratory, University of Michigan, Ann Arbor, Michigan 48109
3. Department of Physics, University of Wisconsin, Madison, WI. 53706
4. Visiting Astronomer, National Solar Observatory, National Optical Astronomy Observatories, which is operated by the Association for Research in Astronomy, Inc., under contract with the National Science Foundation.

ABSTRACT

A set of high resolution Fabry-Perot measurements of the coma of comet P/Halley were acquired in the [O I] 6300 Å and NH_2 6298.62 Å emission lines. These high resolution measurements provide the first optical observations capable of studying directly the photochemical kinetics and dynamic outflow of the coma. The observations were analyzed by a Monte Carlo Particle Trajectory Model. The agreement of the model and observed line profiles was excellent and verified the underlying dynamics, exothermic photodissociative chemistry, and collisional thermalization in the coma. The somewhat wider line profile width for the $O(^1D)$ emission in January 1986 compared to May 1986 is, for example, produced by the larger outflow speed nearer perihelion in January. The January NH_2 profile, which is more narrow than the January $O(^1D)$ profile, is indicative of the outflow dynamics of the parent molecules in the coma. The absolute calibration of the observations in January 1986 allowed the production rates for the H_2O and NH_2 parent molecules to be determined. The average daily water production rates derived from the $O(^1D)$ emission data for January 16 and 17 are, respectively, 2.90×10^{30} molecules s^{-1} and 2.68×10^{30} molecules s^{-1}. These very large water production rates are consistent with the extrapolated (and 7.6-day time variable) water production rates determined from the analysis of lower spectral resolution observations for $O(^1D)$ and Hα emissions (Smyth et al. 1993) that covered the time period up to January 13. The large production rates on January 16 and 17 establish that the maximum water production rate for comet Halley occurred pre-perihelion in January. Implications drawn from comparison with 18-cm radio

emission data in January suggest that the peak water production rate was even larger and might have been as large as ~3.6 x 10^{30} molecules s^{-1} near January 23. The average production rate for NH_3 determined from the NH_2 emission data for January 17 was 1.48 x 10^{28} molecules s^{-1}, yielding a NH_3/H_2O production rate ratio of 0.55%. This ratio is consistent with the range of earlier derived values. The corrected g-value noted in the NH_2 analysis brings most NH_2 production rates in line with NH production rates and also makes them consistent with the production of both species from NH_3.

Subject headings: Comets

1. INTRODUCTION

An important goal of cometary physics is understanding the photochemical kinetics and dynamics of molecules within the coma. Although radio emission lines from the coma have yielded much valuable information on coma gas dynamics, the possibilities of using optical emission lines for this purpose have not been fully explored. The relatively slow speed of cometary molecules leads to very narrow optical emission lines. The resolving power and sensitivity required for measuring the profiles of the very narrow and faint lines is difficult to achieve using conventional grating techniques. However, as shown in this paper, the problem is readily handled using Fabry-Perot spectroscopy.

This paper reports a unique set of high resolution Fabry-Perot measurements of [O I] 6300 Å and NH_2 6298.62 Å emissions from the coma of comet Halley, and its successful interpretation using advanced coma gas dynamic and photochemical models. It provides the first conclusive demonstration that high resolution optical measurements, in addition to radio measurements, are important and powerful means for studying the details of coma gas dynamics. The observations were acquired by the Wisconsin Space Physics Group in January and May 1986 at the McMath-Pierce solar telescope on Kitt Peak. The [O I] 6300 Å line profiles were particularly diagnostic for studying contrasting cometary outflow conditions, since the Halley heliocentric distance in January was small (~0.78 AU) and near perihelion (0.59 AU) so that the H_2O production rate was near its maximum value, while the heliocentric distance in May was

much larger (1.68 AU) so that the H_2O production rate was smaller by approximately an order of magnitude. For comet Halley, these optical measurements are particularly important since they provide water production rates during a critical pre-perihelion period when these rates were near their maximum values, when few measurements with the exception of radio emission observations were made, and when the radio OH measurements are difficult to interpret because of uncertainties in corrections for collisional quenching at high water production rates.

The purpose of the paper is to study the photochemical kinetics and dynamic outflow of the coma of comet Halley by analysis of the high resolution optical observations reported herein. A description of the instrument and observations is given in section 2. The cometary model and the analysis of the observations together with their implications are discussed in section 3. A summary of the results of the paper is presented in section 4.

2. INSTRUMENTATION AND OBSERVATIONS

The instrument used for these observations was a Wisconsin 150 mm dual-etalon, pressure-scanned Fabry-Perot spectrometer installed at the McMath-Pierce solar telescope on Kitt Peak where it could receive light either from the main heliostat or the west auxiliary heliostat. The instrument was used for a variety of observations, most of which were carried out at a medium spectral resolving power of 30,000 (Reynolds et al. 1986; Magee-Sauer et al. 1988, 1989, 1990;

Scherb et al. 1990; Smyth et al. 1993). The conversion of the spectrometer to the high-resolution mode (R = 190,000) for the line profile studies was effected by replacing one medium-resolution etalon with a high-resolution etalon. The general layout of the instrument and modifications are discussed in Scherb et al. (1986) & Roesler et al. (1986). Details important for the present paper are discussed below.

For observations conducted prior to March 1986, the high resolution scans were taken using the main heliostat, which uses a 2.0 m flat to feed a 1.52 m diameter, 82.5m focal length mirror. The sky was imaged through a guider onto a 160 mm focal length lens that imaged the primary mirror on the 3.2 mm diameter (slightly oversized) entrance aperture of the instrument. The light was recollimated for the etalon train by a 762 mm focal length lens. A field lens at the entrance aperture reimaged the sky through the Fabry-Perot collimating lens onto the midplane of the etalon train. With this coupling arrangement, the effective field of view was not crisply defined because of vignetting in the etalon train and the need to mask out a defective region of the high-resolution etalon plates. For the medium resolution studies, in which absolute intensity measurements were a primary objective, spatial scans made by letting a star drift across the field of view were used to map the field response and determine the effective field of view (Magee-Sauer 1988). This mapping was not done for the high resolution observations, and the map for the medium resolution mode cannot be applied to the high resolution mode. However the effective field of view diameter is

reasonably estimated to be 1.0 arcmin, and can be accurately boxed between 1.1 and 0.9 arcmin.

The instrumental spectral profile (ISP) was determined by scanning the 6328 Å line from a stabilized He-Ne laser; it is not expected that the profile was significantly different at 6300 Å. This was corroborated by scans of the CeI 6300.21 Å line from a hollow cathode lamp and by thermospheric temperatures estimated from scans of the airglow 6300 Å line in some of the comet scans. For all high-resolution measurements the etalon spacers were 6.25 mm and 0.472 mm, respectively. This choice gave appropriately high resolution, but left ghosts in the transmission function as high as 10% due to incomplete suppression of the transmission peaks of the high resolution etalon. The relative strengths of the ghosts were measured in a scan of the 6300 Å airglow line and are included in the fit used to measure the cometary and airglow line widths. The observation periods were chosen so that ghosts of the 6300 Å airglow line could be accurately separated from the Doppler-shifted cometary line (see Figure 1).

After March 1986, the optical configuration was changed to accommodate an optional imaging detector used for some of our other programs. In the new arrangement, the sky was imaged on the entrance aperture of the Fabry-Perot system, and the telescope primary was imaged within the etalon train (see Roesler et al. 1986). All of the high-resolution scans with the instrument in this configuration were made using the west auxiliary telescope. The field was cleanly determined by the entrance aperture diameter, and the scale was measured both by

imaging a star field and by timing a star drifting a known distance across the field. The field of view diameter for the May 1986 high-resolution observations was 3.5 arcmin. As before, the instrumental profile was determined with the stabilized He-Ne laser at 6328 Å, with corroborating evidence for its applicability from Ce 6300.21 Å and airglow [O I] 6300 Å line widths. He-Ne laser scans were made with various smaller entrance aperture diameters to confirm that spatial variations in intensity across the field would not noticeably bias the measured profiles.

Observational information for the high-resolution [O I] 6300 Å and NH_2 6298.62 Å scans is summarized in Table 1. All observations were taken with the field of view centered on the comet head. Selected observations are illustrated in Figures 1-3. In Figure 1, a high-resolution [O I] 6300 Å scan obtained on 16 January 1986 is shown. The airglow and comet [O I] 6300 Å emission lines are the prominent features. Other apparent emission features are the combined ghosts from the airglow and comet. At this high resolution, there is no NH_2 contamination of the comet [O I] 6300 Å emission. Figure 2 shows a scan of NH_2 6298.62 Å emission obtained on 17 January 1986, and Figure 3 shows the sum of four [O I] 6300 Å scans obtained on 3 May 1986. In Figure 1 and Figure 3, the comet emissions are clearly wider than the airglow. In Table 2, the field of view and the average full width half maximum (FWHM) for each day of observations in Table 1 are summarized. The spectral resolution of the instrument is also indicated in Table 2 and is more than sufficient to resolve the measured line profiles. The ISP used to determine the spectral resolution was obtained from Gaussian fits to scans of the stabilized He-Ne laser. Two Gaussians were needed

to fit the narrow core and broad wings of the instrumental profile. Gaussians convolved with the appropriate instrumental profiles were fitted to the emission line data in order to determine the FWHM of the measured line profiles given in the last column of Table 2.

Although absolute intensity measurements were not originally planned as part of the high-resolution observations, a scan of the hydrogen Hα line, taken on the Trapezium region of the Orion Nebula on UT 18 January 1986, using the high resolution mode, provides a means of extracting intensities from the Halley [O I] 6300 Å and NH_2 scans taken on 16 and 17 January 1986. The basis for this procedure is an intensity-calibrated, CCD Hα image of the Orion Nebula obtained by Dufour and Hester at Palomar Observatory (Walter, Dufour & Hester 1992). The image is 16 arcmin square with a resolution of 1.192 arcsec per pixel (Walter 1992). We found that the Hα intensities in this image are in good agreement with Hα intensity results from an imaging spectrophotometric study of the Orion Nebula by Pogge, Owen & Atwood (1992, 1993). Corrections for variation of instrumental sensitivity at the different wavelengths of Hα and the comet lines were obtained from earlier observations of the star α CMi (Magee-Sauer et al. 1990; Magee-Sauer 1988). Atmospheric transmission corrections were based on average transmission conditions at Kitt Peak. The Orion scan data were corrected for the effects of the ghosts in the instrumental profile. The overall uncertainties in the comet intensities given in Table 1 are estimates based on uncertainties in the absolute Orion Nebula Hα intensity, atmospheric transmission corrections, and corrections for wavelength dependence of instrumental sensitivity.

3. ANALYSIS OF THE OBSERVATIONS

3.1 Model Description

In order to calculate the high resolution line profiles for both the [O I] 6300 Å and NH_2 6298.62 Å emissions, we have used the Monte Carlo Particle Trajectory Model (MCPTM). For NH_2 and for the OH component of the [O I] 6300 Å emission, the most general heavy species collision algorithm as recently presented by Combi, Bos & Smyth (1993) has been used. This MCPTM is the most recent update to the detailed description provided in previous papers by Combi & Smyth (1988a, b) which had its origins in the first Monte Carlo model by Combi & Delsemme (1980). In the MCPTM, the description adopted for the outflowing collisional inner coma was determined from a hybrid gas-dynamic/Monte Carlo model calculation for H atoms produced photochemically from the H_2O exothermic dissociative chain. In this hybrid calculation, the Monte Carlo model for H atoms was used to compute the photochemical heating efficiency of the coma and was run in an iterative fashion with the dusty-gas dynamic model in order to compute consistently the gas outflow and temperature of the coma for the conditions expected in both the January and May time periods. In the hybrid calculation, a reasonable estimate of the water production rate is required and was obtained from many previously published data. Table 3 shows the model parameters used in the hybrid model calculation. These parameters and the water production rate used are equivalent to those adopted by Combi (1989) and more recently used in the analysis of the February 2-6, 1986, Pioneer Venus

Orbiter UVS image of the H coma of Halley (Smyth, Combi & Stewart 1991). For the purposes of the basic coma modeling, water production rates were used which are accurate to within 20-30%. Differences of a factor of two or more begin to have noticeable effects on the coma velocity and temperature fields, whereas a factor of ten has a large effect (Bockelee-Morvan & Crovisier 1987; Combi 1989). The hybrid model calculations for the variations of the outflow speed and the gas temperature, with distance from the nucleus, are shown in Figures 4a and 4b for both the January 16-17 and May 3-4 epochs. Note the much larger outflow speeds and gas temperatures in January compared with May. These outflow speeds are consistent with various radio observations of OH (Schloerb, Claussen & Tacconi-Garman 1987; Bockelee-Morvan, Crovisier & Gerard 1990) and HCN (Schloerb et al. 1987).

With the conditions of the inner collisional coma determined for the observational dates in January and May, the MCPTM calculations for the observed line profiles can be performed. Line profile information is saved in the MCPTM by accumulating the line of sight component of all atoms or radicals within the projected observational aperture in a set of velocity bins (Schloerb & Gerard 1985; Combi 1989) which were 0.1 km s^{-1} in width in our case. Because of the speed of modern workstations and in order to obtain sufficiently high statistical accuracy, each of the models presented in this paper used 5,000,000 simulation molecules. Full collisional models in a coma of high gas production take only a fraction of an hour to run. Values adopted in the MCPTM for the photodissociation lifetimes of H_2O and OH and for their corresponding branching

ratios that determine the $O(^1D)$ production rate are the same as discussed by Smyth et al. (1993). For NH_2, lifetimes were adopted from the results of the spatial profile analysis of Fink, Combi & DiSanti (1991), who found Haser model parent and daughter scale lengths which were reasonably consistent with production from NH_3 photodissociation. The lifetimes used in the model, reduced to a heliocentric distance of 1 AU, are given in Table 3. The NH_2 lifetimes are an 'average' of the pre- and post-perihelion values found by Fink, Combi & DiSanti, who found a clear asymmetry in both the parent and daughter scale lengths for NH_2.

There exists the possibility, even the likelihood, that when NH_2 is produced in the photodissociation of NH_3 that there will be some excess energy which would be available for translational velocities for the fragments, NH_2 and H. Since we have data only for the January, when the water production rate was quite large, any excess translational velocity of NH_2 would be nearly immediately collisionally quenched. Such behavior has been illustrated by Combi, Bos & Smyth (1993) even for OH which has a much longer parent lifetime and for a case of an even smaller water production rate. We have studied the importance of collisional quenching using the MCPTM and test ejection speeds for NH_2 as large as 1 km s^{-1}. There was no measurable effect for ejection speeds for NH_2. This may not be the case at large heliocentric distances and/or lower water production rates. Tegler (1992) has suggested a translational ejection for NH_2 on the order of 0.5 km s^{-1}.

3.2 Line Profile Analysis

The appearance of line profiles from various types of simple coma outflow models has been recently discussed in a paper by Bockelée-Morvan, Crovisier & Gerard (1990). They show, for example, that a classical 'vectorial' type model produces a trapezoidal shaped line profile. Combi (1989) showed line profiles resulting from more physically realistic modeled comae that included the intrinsic variation of outflow speed with increasing distance from the nucleus and the gas temperature. These effects tend to make the unusual looking profiles appear more Gaussian. Real observed profiles are furthermore convolved with the ISP, that is here approximated by two Gaussians, and that under the best of circumstances has a width nearly as large as the intrinsic width of the coma line in question. For the analysis presented here, the ISP was determined from scans of the helium-neon spectral laser and was convolve with coma model line profiles. Nonetheless, it is instructive to examine the shape of model line profiles before convolution with the ISP. For the $O(^1D)$ profile it is also useful to examine the appearance of the H_2O and OH sources of $O(^1D)$ atoms separately.

Figure 5a shows the $O(^1D)$ emission line profile corresponding to the average conditions for January 16-17 before convolution with the ISP. Figure 5b shows a similar plot for May 3-4. Shown are the separated contributions from the H_2O and OH sources as well as the sum, weighted according to the branching ratios given in Table 3. In both cases the H_2O source dominates the emission within the aperture, because in both cases most of the water in the coma is within the aperture but most of the OH is outside. The aperture was larger in May

compared with January, but proportionally smaller compared with the much larger photodecay lifetime of water, so that the relative OH-source contribution was even smaller, as shown. If the entire coma were observed, the OH source would actually be nearly twice that of the H_2O source. The profile from the OH source is somewhat wider than that from H_2O because of the additional 1.05 km s^{-1} the OH receives upon dissociation from water. This is counteracted slightly by the ejection speed of the $O(^1D)$ atoms which is actually slightly smaller from OH than from H_2O (1.5 vs. 1.6 km s^{-1}).

Figures 6 a&b show an example of the effects of the ISP convolution on the modeled profiles for $O(^1D)$ and NH_2 in January. The slight apparent offset of the intrinsic cometary and ISP convolved profile is due to the fact that the actual ISP from the He-Ne laser was slightly asymmetric. The ISP causes the final observed profile to appear very Gaussian like, and removes any peculiar or interesting features that the profile could show if observed at a substantially higher spectral resolution.

The agreement between modeled and observed line profiles is excellent. Figures 7 a&b show observed $O(^1D)$ profiles from January and May compared with the model profiles for the combined H_2O and OH sources convolved with the ISP. For the May data we have summed all of the profiles observed on May 3 and 4 to improve signal-to-noise. The somewhat wider January profile is naturally explained by the larger outflow speed as predicted by the gas-dynamic/Monte Carlo model (Figures 4 a&b). Figure 8 shows the observed NH_2

profile from January 17 compared with the comparable model again convolved with the ISP. Because of the combination of the high water production rate and short lifetime for the NH_2 parent (NH_3), the width and shape of the NH_2 profile should be indicative of the outflow speed and temperature for parent molecules (H_2O). As mentioned above, especially for the January coma conditions, we expect there to be no measurable effect from any photodissociative ejection velocity for NH_2, if one exists, because of collisional quenching. The slight misalignment (≤ 0.2 km s^{-1} or ≤ 4 mÅ) of the center of the model and observed line profiles in Figures 7a and 8 (i.e., the model profiles need to be moved slightly to the left in the January data) and in Figure 7b (i.e., the model profile needs to be moved slightly to the right in the May data) is likely due to small motions typical in the earth's atmosphere. These motions cause the center of the terrestrial $O(^1D)$ line profile, used to determine the absolute wavelength scale for the observations, to vary slightly.

In order to investigate the sensitivity of the profiles to changes in model parameters, we have also compared a number of simple Monte Carlo/vectorial models, i.e. models with single values of the parent molecule and ejection speeds for the daughters, for a range of outflow speeds, and convolved them with the ISP. It is clear that outflow speed differences more than 0.2 km s^{-1} are quite significant and that such differences between the model and measurement would be easily detectable in data-model comparisons. The outflow speed differences between January and May are larger than this (see Figures 4 a&b).

3.3 Production Rates

In addition to the line profile information, as mentioned above, an absolute calibration was possible for all January observations in Table 1. With this information, it was possible to use the model results to calculate NH_3 and H_2O production rates. The MCPTM simulates the coma by using a large number of molecules (5 million in this case for good statistical coverage) that are ejected into the coma over a long enough time (2×10^6 seconds) so that the model coma relaxes to a realistic steady-state condition. All of the computed quantities in the model (e.g., abundances) are normalized to the simulation production rate, which is the number of simulation molecules divided by the total simulation run time. Simulation quantities are calculated per unit production rate and can then be converted to physical quantities by multiplying by the actual production rate. For any decaying species, produced at a constant rate, the sum of all particles in the coma is simply the product of the production rate and the lifetime of the species. Since the model is normalized to a unit production rate, the total number of simulated molecules (or radicals) in the coma is equal to the lifetime of that species. In the models for the analyses presented here, the total number of simulation radicals within the aperture is obtained simply by integrating over the line profile. When this number is multiplied by the production rate, the number of actual radicals within the aperture is obtained.

For the case of NH_2, the total number of radicals in the aperture, times the fluorescence rate (or g-factor), in photons per second per radical into 4π steradians, times 10^{-6}, yields the intensity in Rayleighs. Since the brightness is

observed, the production rate is the only unknown and can be calculated. The absolute value of the fluorescence rates for the various bands of NH_2 has been a contentious issue in the last several years. In the pre-Halley review paper by A'Hearn (1982), the g-factors for the (0,7,0) through (0,12,0) NH_2 bands were summarized as computed in an earlier paper (A'Hearn, Hanich & Thurber 1980). This was the result of a simple calculation assuming that fluorescence occurs in each band individually from the ground state. Tegler & Wyckoff (1989) performed a more sophisticated calculation extending to more bands, (0,3,0) through (0,15,0), and using updated experimental data and theoretical transition probabilities. The newer g-values were smaller by factors of 1.4 to 5.9. Most importantly for our purposes here, the g-value for the (0,8,0) band decreased from 1.694×10^{-2} to 4.95×10^{-3} photons per second. Such a change would increase NH_2 production rates determined from (0,8,0) band observations by a factor of more than three. Finally, the "Note added in proof" in the paper by Magee-Sauer et al. (1989), quotes Arpigny as finding that there are Ka"=1 levels which are not sampled by the (0,8,0) band. This results in "hidden" NH_2, if one were to determine NH_2 abundances from (0,8,0) band observations alone. The effect is about a factor of 2, which would bring the g-value down even further to 2.475×10^{-3} photons per radical per second into 4π steradians. This extra factor of 2 brings most NH_2 production rates in line with NH production rates (Schleicher & Millis 1989; Feldman et al. 1993) and makes them consistent with production of both species from NH_3. Using this g-value, the NH_2 production rates determined from the 17 January 1986 high-resolution observations are

summarized in Table 4. The average NH_2 production rate for 17 January was 1.48×10^{28} molecules s^{-1}.

For the case of $O(^1D)$, the calculation of a water production rate is more complicated, but still relatively straightforward. Since the $O(^1D)$ emission is a spin-forbidden transition it does not emit by fluorescence but rather as a result of photodissociation of a fraction of H_2O, producing H_2 +$O(^1D)$, and a fraction of OH, producing H + $O(^1D)$. The best estimate for the branching ratio from the H_2O source is from Smyth et al. (1993) for the quiet sun conditions relevant for the Halley time period. This value is consistent with the earlier estimate of Combi & Smyth (1988b). Since the OH lifetime is dominated by predissociation in the near UV (Schleicher & A'Hearn 1988) and is highly dependent on the heliocentric velocity of the comet, the branching ratio actually varies even though the rate for the far UV component that is responsible for the $O(^1D)$ production (van Dishoeck & Dalgarno 1984) does not vary with heliocentric velocity. For January 16 and 17 the average heliocentric velocity was -23.3 km/s. The values of all of the relevant branching ratios and lifetimes are given in Table 3.

The brightness of $O(^1D)$ per unit production rate was calculated from the MCPTM given the total abundances of H_2O and OH within the aperture (which were obtained by integrating over the line profiles) times the total production rate of $O(^1D)$ atoms from each parent species times 10^{-6} to get brightness units of Rayleighs. These rates, which are defined in Table 3, are given as $\nu(H_2O)=(BR2)/\tau_1$ and $\nu(OH)=(BR1)(BR3)/\tau_2$. Finally, one needs to account for

the 3 to 1 ratio between the two lines of the ^1D to ^3P doublet at 6300 and 6364 Å, respectively. This introduces a factor of 3/4 of a 6300Å photon emitted per O(^1D) atom produced. The calculated H_2O production rates determined in this manner from the O(^1D) observations are given in Table 5. The water production rates in Table 5 are quite high. The average value on January 16 is 2.90 x 10^{30} molecules s^{-1}, and the single value on January 17 is 2.68 x 10^{30} molecules s^{-1}. These values are in fact the highest water production rates yet reported for comet Halley, higher even than those right around perihelion (Smyth, Combi & Stewart 1991; Smyth, Marconi & Combi 1993).

3.4 Halley's Activity in January 1986

Because of its close proximity to the sun in the sky during January 1986, most ground-based optical observations of the comet stopped by January 12 or 13 (Schleicher et al. 1990, Fink, Combi & DiSanti 1991, Smyth et al. 1993). Therefore, there are little directly comparable data with which to compare our production rates from January 16 and 17. In order to provide a check on the validity of these large water production rates, we have, however, compared these values with the published medium spectral resolution values from January 4 through 13 recently reanalyzed by Smyth et al. (1993) and shown to be consistent with a comparable set of H Balmer-α observations. In addition, we have also compared those early January water production rates with a nearly simultaneous set of C_2 production rates to examine the correlation of day-to-day changes in production rates between species and how the expected 7-plus day periodicity in

those data (Schleicher et al. 1990) might extrapolate to the production rates on January 16 and 17.

To facilitate this extrapolation, it is important first to compare the earlier water and C_2 production rates. Figure 9 shows the production rates of water from January 4 through 13 in the analysis of medium-spectral-resolution O(^{1}D) and Hα observations of Smyth et al. along with the C_2 production rates during the same period published by Schleicher et al. and with new unpublished C_2 rates very recently obtained from Schleicher (1993) for January 11, 14 and 18 (i.e., days from perihelion of about -29, -26 and -22). These three points were corrected so as to be consistent with the C_2 scale lengths used previously by Schleicher et al. (1990). From day -38 to -27 where the data coverage is almost daily, it is clear that the same general day-to-day time variation of the C_2 production rate is evident in the water production rate determined from the O(^{1}D) and Hα observations. The photometry was not abundant enough for Schleicher et al. to derive a very good period for January 1986 alone. When grouping all C_2 data from November 1985 through January 1986, Schleicher et al. found an optimal value of 7.46 days. This is in contrast to 7.60 days for their March data (which included late February through mid-March) and 7.37 days for their April data (which included late March through late April). Combi & Fink (1993), furthermore, showed that the analysis of spatial profiles from March 1 and 2 --- during a data gap in the photometry --- required the use of the 7.60 day period as contrasted with the 7.37-day period. They also noted that the day-to-day variations of the water production rates as calculated from the Pioneer Venus

Orbiter observations (Stewart 1987) clearly showed that the same 7.6-day "March-lightcurve" was repeating at least as far back as the time of perihelion (February 9).

The daily averaged water production rates for January 16 and 17 in Figure 9 (filled circles) lie only slightly higher than the trend set by the early January water production rates noted in Figure 9. If the C_2 production rates are multiplied by 832, they match the water production rates very well from day -38 to -27 where the data coverage is almost daily. An extrapolation of these rates for later times was then accomplished by shifting them ahead by 7.60 days and adjusting them upwards by the heliocentric distance trend ($r^{-3.25}$) of the C_2 data. This extrapolation is shown in Figure 10 where the water production rates determined from the Hα data have not been included for clarity. The January 16 and 17 points are seen to be only slightly higher than the extrapolated pattern and have the proper relative values with respect to the time dependent 7.6 day extrapolated pattern seen a week earlier around January 8 and 9. The high resolution point on January 16 falls just after the peak seen in the extrapolated medium resolution data on January 8. Examination of the individual C_2 light curves for different 7-plus day periods (Schleicher et al. 1990) shows two different time patterns for the maximum amplitude, the larger of which is very similar to the pattern produced by the two water production rates on January 16 and 17. We conclude that the water production rates on January 16 and 17, although large, are very reasonable and have values similar to those expected from extrapolating earlier data.

A comparison of the average H_2O production rates derived from the high resolution O(^{1}D) observations on January 16 and 17 with other H_2O production rates is presented in Figure 11. As noted in Figure 9, the water production rates on January 16 and 17 (• symbols) appear to be a continuation of the rates determined from the O(^{1}D) data (□ symbols) and Hα data (∇ symbols) of Smyth et al. (1993) which were acquired up to January 13. From this comparison, the importance of the pre-perihelion peak in the water production rate can be appreciated even though there is a gap in the daily coverage (with the exception of the radio emission data, × symbols) from January 18 to January 31, where the Pioneer Venus H Lyman-α measurements (+ symbols) then begin on February 1. The largest production rate near perihelion determined from the Pioneer Venus H Lyman-α measurements is 1.8×10^{30} molecules s^{-1}, which is a factor of 1.6 smaller than the 2.90×10^{30} molecules s^{-1} value determined for January 16. The water production rate was, however, likely even larger in later January since its rapid rise, which in Figure 11 began about January 10 and is still evident on our last data point on January 17, shows no change in its steep upward slope. The water production rates derived from the 18-cm radio emission data (× symbols) fill in this gap, but are much smaller than the water production rates determined from optical and ultraviolet observations on either side of the gap by about a factor of 3. The factor of 3 is most likely caused by uncertainties in correcting the radio data for collisional quenching at these very high water production rates. If the water production rates for the radio emission data in the region of the gap are multiplied by a factor of three, their steady increase and then decrease in this gap would imply that the water production rate reached a pre-perihelion maximum

near January 23 of about 3.6 x 10^{30} molecules s^{-1}. Further efforts to improve the collisional quenching correction of the radio emission data are clearly important to refine this pre-perihelion behavior for the water production rate. In additional to these O(^{1}D) results, our reasonable values for the implied NH_3/H_2O production rate ratio (see below) places more certainty on the surprisingly large value of the pre-perihelion water production rate.

3.5 The NH_3/H_2O Production Rate Ratio

The yield of NH_2 from NH_3 photodissociation is about 95%. Most of the NH_2 is subsequently photodissociated and yields mostly NH, which is also observed in comets. There has been some controversy in the last couple of years regarding NH_3 production in comets in general and in Halley, in particular. The major discrepancies have been due mostly to uncertainties and overestimates of the NH_2 g-factor, although there is some degree of uncertainty from the NH lifetime and/or parent and daughter Haser scale lengths which are used in the analysis of NH observations. Recently, Arpigny et al. (1993) reported that most estimates of the NH_3/H_2O ratio from both NH and NH_2 observations in Halley are consistent with values somewhat less than but near 1%. Given the latest and best estimates for both the O(^{1}D) branching ratios and the NH_2 g-factors, our value for the NH_3/H_2O ratio on 17 January is 0.55%. The average value determined from the medium resolution data of Magee-Sauer et al. (1989) for January 1986, corrected for the Tegler & Wyckoff (1989) band emission rates and the factor of 2 from Arpigny (see note in Magee-Sauer et al.), was 0.75%.

Other determinations for the NH_3/H_2O ratio from NH_2 observations in Halley are 0.1-0.7% by Wyckoff et al. (1988) and 0.3% by Fink (1993). All these have been renormalized to the same g-factor. A value determined from NH observations is 0.44-0.94% by Feldman et al. (1993). Schleicher & Millis (1989) have published a value of 0.5% for a 'normal comet' as determined from aperture photometry of comets P/Halley, P/Borrelly & Liller (1988a). Feldman et al. (1993) present values of the NH/OH ratio in a number of comets observed with IUE to be in the range of 0.39-0.95%. These would imply NH_3/H_2O ratios in the range of 0.36-0.88%. Finally, all of these 'measured' NH_3/H_2O ratios depend on the models and model parameters employed in their respective analyses; the analyses are far from uniform. Despite the nonuniformity of analysis, it is likely that both NH and NH_2 observations are consistent with production from NH_3 in the range of 0.4 to 1.0% of that of water. Our value of 0.55% fits well within this range.

4. SUMMARY

The first high spectral resolution optical observations for the coma of comet Halley capable of studying the photochemical kinetics and dynamics of outflowing molecules were acquired in 1986 for [O I] 6300 Å and NH_2 6298.62 Å emissions in the January pre-perihelion time frame and also for [O I] 6300 Å emissions in the May post-perihelion time frame. The measured line profiles were obtained for apertures centered on the nucleus, and an absolute calibration of the emission line brightnesses in January was determined. The observations were

analyzed by employing the MCPTM of Combi & Smyth (1988a, b), using the recent heavy species collisional algorithm of Combi, Bos & Smyth (1993) for NH_2 and the OH component of [O I] 6300 Å emission.

The agreement of the model line profiles with the observations in January of O(^{1}D) and NH_2 and in May of O(^{1}D) was excellent and represents yet another in a series of verifications in the last several years of the modeling techniques and physical parameters employed. Model simulations show that outflow speed differences more than ~0.2 km s^{-1} are quite significant and that such differences between the model and measurement would be easily detectable in data-model comparisons. The somewhat wider line profile width for the O(^{1}D) emission in January compared to May is produced by the larger outflow speed nearer perihelion in January. Doppler broadening of the NH_2 line profiles because of the (expected, but yet undetermined) translational velocity imparted to NH_2 from its exothermic NH_3 photodissociation was shown in model simulations to be collisionally quenched for molecules in the observing aperture (i.e., 0.5 arcmin from the nucleus) and hence unimportant. For the O(^{1}D) line profile, the translational velocities imparted to O(^{1}D) upon exothermic dissociation of H_2O and OH are not collisionally quenched and do play a role in the line profile width. The separate contributions to the O(^{1}D) emission line profile produced by the photodissociation of H_2O and OH were calculated and discussed, and the composite line profile was constructed by their properly weighted sum. The profile contribution from OH is somewhat wider than from H_2O because of the additional 1.05 km s^{-1} that OH receives upon dissociation from water. The

convolution of the composite modeled line profile with the instrumental spectral profile, however, causes the final observed profile to appear very Gaussian like and removes any interesting features that the profile could show if observed at a substantially higher spectral resolution.

The absolute calibration for the observations in January allows the production rates for the H_2O and NH_3 parent molecules to be calculated. The average water production rates derived from the O(^{1}D) emission data for January 16 and 17 are, respectively 2.90 x 10^{30} molecules s^{-1} and 2.68 x 10^{30} molecules s^{-1}. These very large water production rates are consistent with the extrapolated (and 7.6-day time variable) water production rates determined from the analysis of medium spectral resolution observations for O(^{1}D) and Hα emissions (Smyth et al. 1993) that covered the time period from January 4-13, 1986. Together with the water production rates derived from the analysis of medium spectral resolution observations, these large production rates on January 16 and 17 establish that the maximum water production rate for comet Halley occurred pre-perihelion in January. The previously largest water production rate determined from the H Lyman-α observations for times very near perihelion was 1.8 x 10^{30} molecules s^{-1}, which is a factor of 1.6 times smaller than the value on January 16. Although there are difficulties (as illustrated in this paper) in determining the absolute water production rate from the 18-cm radio emission data acquired in January and early February because of correcting for collisional quenching, the peak water production rate may be ~3.6 x 10^{30} molecules s^{-1} and occur near January 23 if they are approximately scaled by a factor of three using optical and ultraviolet

data as a guide. However, to do this scaling properly, a careful reassessment of the collisional quenching calculation would need to be done for the cometary plasma conditions appropriate for small heliocentric distances and large production rates. The average production rate for NH_3 determined from the NH_2 emission data for January 17 was 1.48×10^{28} molecules s^{-1} and produced a NH_3/H_2O production rate ratio of 0.55%. This ratio is consistent with the range of earlier derived values and therefore provides independent support for the high water production rates derived from the $O(^1D)$ emission data in January. The corrected g-value noted in the NH_2 analysis brings most NH_2 production rates in line with NH production rates and also makes them consistent with the production of both species from NH_3.

ACKNOWLEDGMENTS

We wish to thank J. Harlander and K. Magee-Sauer for assistance with the observations, and the staff of the National Solar Observatory for their generous support. We are most indebted to D. Walter and J. Hester for providing photometrically calibrated images of the Orion nebula, without which the absolute intensity calibrations of the January measurements would not be possible. We also wish to thank D. Schleicher for providing new C_2 photometry data before publication. This research was supported by the Planetary Atmospheres Program of the National Aeronautics and Space Administration under grant NAGW-1946 to the University of Michigan and under contracts NASW-4329 and NASW-4496 to Atmospheric and Environmental Research, Inc. It was also supported by the Planetary Astronomy Program of the National Aeronautics and Space Administration under grants NAGW-695 and NAGW-3319 to the University of Wisconsin.

REFERENCES

A'Hearn, M. F. 1982, in Comets, ed. L.L Wilkening (Tucson: Univ. of Arizona Press), 433

A'Hearn, M. F., Hanich, R. J., & Thurber,.C. H. 1980, AJ, 85, 74

Arpigny, C., Weaver, H. A., A'Hearn, M. F., & Feldman, P. D. 1993, Presented at Asteroid, Comets and Meteors 1993, in Belgirate, Italy, June 14-18

Bockelee-Morvan, D.& Crovisier, J. 1987, ESA, SP-278

Bockelée-Morvan, D., Crovisier, J., & Gerard, E. 1990, A&A, 238, 382

Combi, M. R. 1989, Icarus , 81, 41

Combi, M. R., & Delsemme, A.H. 1980, ApJ, 237, 633

Combi, M. R., & Fink, U. 1993, ApJ, 409, 790

Combi, M. R., & Smyth, W. H. 1988a, ApJ, 327, 1026

Combi, M. R., & Smyth, W. H. 1988b, ApJ, 327, 1044

Combi, M. R., Bos, B. J., & Smyth, W. H. 1993, ApJ, 404, 668

Feldman, P. D., Fournier, K. B., Grinin, V. P., & Zvereva, A. M. 1993, ApJ, in press

Fink, U. 1993, ApJ, in press

Fink, U.& DiSanti, A. 1990, ApJ, 364, 687

Fink, U., Combi, M. R., & DiSanti, M.A. 1991, ApJ, 383, 356

Magee-Sauer, K. P. 1988, Ph.D. Thesis, Univ. of Wisconsin, Madison

Magee-Sauer, K., Roesler, F. L., Scherb, F. & Harlander, J. 1988, Icarus, 76, 89

Magee-Sauer, K., Scherb, F., Roesler, F. L. & Harlander, J. 1989, Icarus, 82, 50

Magee-Sauer, K., Scherb, F., Roesler, F. L. & Harlander, J. 1990, Icarus, 84, 154

McCoy, R. P., Meier, R. R., Keller, H. V. & Carruthers, G. R. 1992, A&A, 258, 555

Pogge, R. W., Owen, J. M., & Atwood, B. 1992, ApJ, 399, 147

Pogge, R. W., Owen, J. M., & Atwood, B. 1993, ApJ, 408, 758

Reynolds, R. J., Magee, K., Roesler, F. L., Scherb, F., & Harlander, J. 1986, ApJ, 309, L9

Roesler, F. L., Scherb, F., Magee, K., Harlander, J., Reynolds, R. J., Yell, R. V., Broadfoot, A. L., & Oliversen, R. J. 1986, Adv. Space Res., 5, 279

Scherb, F., Magee-Sauer, K., Roesler, F. L., & Harlander, J. 1990, Icarus, 86, 172

Scherb, F., Roesler, F. L., Magee, K., Harlander, J., & Reynolds, R. J. 1986, Adv. Space Res., 5, 275

Schleicher, D. G. 1993, private communication

Schleicher, D. G., & A'Hearn, M. F. 1988, ApJ, 331, 1058

Schleicher, D. G., & Millis, R. L. 1989, ApJ, 339, 1107

Schleicher, D. G., Millis, R. L., Thompson, D. T., Birch, P. V, Martin, R. M., Tholen, D. J., Piscitelli, J. R., Lark, N. L., & Hammel, H.B. 1990, AJ, 100, 896

Schloerb, F. P & Gerard E. 1985, ApJ, 90, 1117

Schloerb, F. P., Claussen, M. K., & Tacconi-Garman, L. 1987, A&A, 187, 469

Schloerb, F. P., Kinzel, W. M., Swade, D. A. & Irvine, W. M. 1987, A&A, 187, 369

Smyth, W. H., Combi, M. R. & Stewart, A. I. F. 1991, Science, 253, 1008

Smyth, W. H., Marconi, M. L. & Combi, M. R. 1993, Icarus, submitted

Smyth, W. H., Marconi, M. L., Scherb, F., & Roesler, F. L. 1993, ApJ, 413, 756

Stewart, A. I. F. 1987, A&A, 187, 369

Tegler, S. 1992, private communication

Tegler, S., & Wyckoff, S. 1989, ApJ, 343, 445

van Dishoeck, E. F., & Dalgarno, A. 1984, Icarus, 59, 305

Walter, D. K. 1992, private communication

Walter, D. K., Dufour, R. J., & Hester, J. J. 1992, ApJ, 397, 196

Wyckoff, S., Tegler, S., Wehinger, P., Spinrad, H. & Belton, M. 1988, ApJ, 325, 927

Table 1

Log of High-Resolution Comet Halley Scans

UT Date of Observation	Start Time (UT)	Total Scan Time (minutes)	Species and Emission Wavelength (Å)	Z^a (degrees)	Airmass	$R_h{}^b$ (AV)	Δ^c (AU)	I^d (Rayleighs)
1986 January 16	0132	7.1	[OI] 6300.3	68.0	2.7	0.79	1.42	2,240 ± 310
	0141	7.1	[OI] 6300.3	69.7	2.9	0.79	1.42	2,270 ± 320
	0150	7.1	[OI] 6300.3	71.8	3.2	0.79	1.42	2,260 ± 320
	0200	7.1	[OI] 6300.3	73.4	3.5	0.79	1.42	2,320 ± 320
	0210	3.3	[OI] 6300.3	75.7	4.0	0.79	1.42	2,210 ± 310
	0215	3.2	[OI] 6300.3	76.7	4.3	0.79	1.42	2,200 ± 310
	0221	3.3	[OI] 6300.3	77.9	4.8	0.79	1.42	2,200 ± 310
	0225	3.3	[OI] 6300.3	79.0	5.2	0.79	1.42	2,430 ± 340
	0230	3.2	[OI] 6300.3	79.7	5.6	0.79	1.42	2,390 ± 330
	0235	3.3	[OI] 6300.3	80.5	6.0	0.79	1.42	2,170 ± 300
1986 January 17	0204	8.1	NH_2 6298.6	75.8	4.1	0.77	1.43	990 ± 140
	0215	3.0	NH_2 6298.6	77.9	4.8	0.77	1.43	940 ± 130
	0219	3.0	NH_2 6298.6	78.7	5.1	0.77	1.43	800 ± 110
	0223	3.0	NH_2 6298.6	79.6	5.5	0.77	1.43	900 ± 130
	0228	3.4	[OI] 6300.3	80.6	6.1	0.77	1.43	2,100 ± 290
1986 May 3	0436	6.4	[OI] 6300.3	51.7	1.6	1.66	0.86	
	0446	5.1	[OI] 6300.3	52.5	1.6	1.66	0.86	
	0452	5.0	[OI] 6300.3	53.0	1.7	1.66	0.86	
	0506	8.3	[OI] 6300.3	54.2	1.7	1.66	0.86	
1986 May 4	0305	15.7	[OI] 6300.3	48.2	1.5	1.68	0.89	
	0322	7.1	[OI] 6300.3	48.0	1.5	1.68	0.89	
	0331	7.0	[OI] 6300.3	48.0	1.5	1.68	0.89	

a Zenith angle of observation
b Heliocentric distance
c Geocentric distance
d Average intensity over the field of view.

Table 2

Observational Information for the Wisconsin High Resolution $O(^1D)$ and NH_2 Line Profiles

Species (Wavelength, Å)	UT Date	Field of View Diameter (arcmin)	Field of View Radius (10^4 km)	Spectral Resolution (km sec^{-1})	FWHM Gaussian Fit (km sec^{-1})
OI (6300.30)	16 Jan. '86	1.0 ± 0.1	3.1 ± 0.3	1.30	3.22 ± 0.13
	17 Jan. '86	1.0 ± 0.1	3.1 ± 0.3	1.45	2.90 ± 0.11
	3 May '86	3.5	6.6	1.71	2.73 ± 0.28
	4 May '86	3.5	6.8	1.66	2.07 ± 0.18
NH_2 (6298.62)	17 Jan. '86	1.0 ± 0.1	3.1 ± 0.3	1.45	2.48 ± 0.11

Table 3

Parameters for the Hybrid Gas-dynamic/Monte Carlo Coma Model

January 16 17 Gas Production Rate = 1×10^{30} s^{-1}

May 3-4 Gas Production Rate = 1×10^{29} s^{-1}

Radical-H_2O collisional cross section = 3.5×10^{-15} cm^{-2}

H_2O lifetime: $\tau_1 = 8.2 \times 10^4$ seconds at 1 AU

OH lifetime: $\tau_3 = 1.23 \times 10^5$ seconds at 0.78 AU (January 16-17 average)

$\tau_3 = 4.07 \times 10^5$ seconds at 1.68 AU (May 3-4 average)

NH_3 lifetime: 7.0×10^3 seconds at 1AU

NH_2 lifetime: 5.0×10^4 seconds at 1 AU

Branching Ratios: BR1=OH from H_2O = 0.88

BR2=O(^{1}D) from H_2O = 0.034

BR3=O(^{1}D) from OH = 0.081

Table 4

Production Rate of NH_2 from 6298.6 Å Line Profiles

UT Date of Observation	Start Time (UT)	Average Intensity (Rayleighs)	Production Rate of NH_2 (10^{28} molecules s^{-1})
1986 January 17	0204	990 ± 140	1.62 ± 0.23
	0215	940 ± 130	1.53 ± 0.21
	0219	800 ± 110	1.29 ± 0.18
	0223	900 ± 130	1.47 ± 0.21

Table 5

Production Rate of Water from [O I] 6300Å Line Profiles

UT Date of Observation	Start Time (UT)	Average Intensity (Rayleighs)	Production Rate of Water (10^{30} molecules s^{-1})
1986 January 16	0132	2240 ± 310	2.86 ± 0.40
	0141	2270 ± 320	2.91 ± 0.41
	0150	2260 ± 320	2.90 ± 0.41
	0200	2320 ± 320	2.95 ± 0.41
	0210	2210 ± 310	2.82 ± 0.39
	0215	2200 ± 310	2.81 ± 0.39
	0221	2200 ± 310	2.81 ± 0.39
	0225	2430 ± 340	3.10 ± 0.43
	0230	2390 ± 330	3.07 ± 0.43
	0235	2170 ± 300	2.77 ± 0.39
1986 January 17	0228	2100 ± 290	2.68 ± 0.38

Figure Captions

FIG. 1. Scan of [O I] 6300 Å Emission, 1986 January 16, 0132 UT. The cometary and airglow emission line profiles are well separated and spectrally resolved. The airglow ghosts fall on either side of the comet [O I] 6300 Å emission. The location of the zero on the velocity scale is arbitrary and has been chosen to be at the center of the cometary emission line.

FIG. 2. Scan of NH_2 6298.62 Å Emission, 1986 January 17, 0204 UT. The cometary NH_2 emission line profile is spectrally resolved and centered on the zero of the velocity scale.

FIG. 3. Sum of Four Scans of [O I] 6300 Å Emission, 1986 May 3, 0204-0226 UT. The cometary and airglow emission line profiles are well separated and spectrally resolved. Relative to the airglow emission line, the cometary emission line is much weaker in May than in January 1986 because of the smaller H_2O production rate of the comet and the larger field of view of the instrument.

Fig. 4. Results of the Gas-dynamic/Monte Carlo Model for Comet P/Halley in January and May 1986. Shown are the variations with distance from the nucleus of the coma outflow speed in (a) and of the gas temperature in (b) for conditions in mid-January and early May 1986. Curves are cut off at the reasonable limits of the hydrodynamic calculation. Note the much higher velocities and gas temperatures in January owing to both the higher heating rate

and the higher degree of collisional thermalization of the hot superthermal H atoms that are largely responsible for the photochemical heating of the coma. The effects of the higher velocities and temperatures are clearly seen even in the Gaussian widths of the O(^{1}D) lines given in Table 2.

Fig. 5. Model for the H_2O and OH Source Components of the O(^{1}D) Line Profile. Model results for the intrinsic O(^{1}D) cometary line profiles for conditions in January are shown in (a) and those in May are shown in (b). In both cases the lowest profile is from the OH source, the middle is from the H_2O source and the highest is the appropriately weighted sum. The instrument spectral profile (ISP) has not been convolved. Note that the OH source is somewhat wider than the H_2O source, but that the H_2O source is dominant for these nucleus-centered apertures. The line profiles were binned in 0.1 km s^{-1} intervals.

Fig. 6. Convolution of Intrinsic Cometary Line Profiles with ISP. The effect of the convolution of the ISP with the intrinsic cometary line profile shapes is illustrated. Shown in (a) is the O(^{1}D) line and in (b) the NH_2 6298.6 line for January 1986 conditions. In both cases the lines with the higher peaks, irregularities and more "interesting" shapes, are the intrinsic cometary line profiles. The ISP tends to broaden a line and make it appear more Gaussian. In each case the lines have been normalized to the same integrated line flux. A slight asymmetry between the lines is caused by the slightly asymmetric ISP.

Fig. 7. Model-Data Comparison for the [O I] 6300 Å Line Profile. Shown in (a) is the observed line profile for January 17 (the histogram) plotted with the ISP-convolved model line profile (smooth curve) and normalized to one another according to the integrated line flux. The feature centered at about +5 km s^{-1} is a ghost in the data which has been properly removed in model-data normalization. Shown in (b) is a similar comparison for the average of the May 3 and 4 observations. See text for a detailed discussion.

Fig. 8. Model-Data Comparison for the NH_2 6298.6 Å Line Profile. The average of the four observed line profiles acquired on January 17 (the histogram) is plotted together with the ISP-convolved model line profile (smooth curve) and normalized to one another according to the integrated line flux.

Fig. 9. Coma Activity of Comet P/Halley in January 1986. Shown are our two new water production rates determined from the high resolution O(^{1}D) line profiles (plotted as filled circles) compared with those determined from the medium resolution O(^{1}D) profiles (open circles) and hydrogen Balmer-α (triangles) from Smyth et al. (1993). Also shown for comparison are the C_2 production rates x 100 (open squares) from Schleicher et al. (1990) and newer values x 100 (filled squares) from Schleicher (1993). It is clear that the day-to-day structure of coma activity was the same in water, from O(^{1}D), as it was in C_2. There are unfortunately no corroborating data in the January 16-17 time period.

Fig. 10. Comparison of the Water Production Rates from High Resolution Line Profiles with an Extrapolated Periodic Light Curve. The two new water production rates determined from the high resolution O(^{1}D) line profiles (plotted as filled circles) are compared with the trend set by the earlier medium resolution values (Smyth et al. 1993) which are shifted by 7.60 days and extrapolated according to the heliocentric distance power law. The original O(^{1}D) medium resolution data from Smyth et al. (1993) are plotted as open circles. The original C_2 data are plotted by open squares and filled squares. The extrapolated O(^{1}D) data are plotted as shaded open circles, and the extrapolated C_2 data are plotted by shaded open squares and shaded filled squares. The two new values coincide reasonably well with the January 8 peak, shifted and extrapolated ahead by 7.6 days.

Fig. 11. Comparison of the Water Production Rates for Comet Halley. The production rates in units of 10^{29} molecules/s are shown as a function of the day of the year from November 1985 to May 1986 for a variety of measurements. The day of perihelion is shown by the vertical dotted line. The symbols refer to the following: (Δ) H_2O production rates determined from IUE data for OH emission by Combi, Bos & Smyth (1993); ($\square$) H_2O production rates determined from the revised analysis (Smyth et al. 1993) of the 6300Å emission data for atomic oxygen originally published by Magee-Sauer et al. (1990); (∇) H_2O production rates determined from the analysis of Hα emission data by Smyth et al. (1993); ($\times$) H_2O production rates determined from 18-cm OH radio observations by Bockelée-Morvan, Crovisier, & Gerard (1990); ($\diamond$) H_2O

production rates determined from rocket observations of H Lyman-α emission by McCoy et al. (1992); (*) H_2O production rates determined from [O I] 6300 Å emission observations of atomic oxygen by Fink & DiSanti (1990); (+) production rates determined from the H Lyman-α observations of Smyth, Marconi & Combi (1993); (•) average daily H_2O production rates determined in this paper from the [O I] 6300 Å emission observations in Table 1.

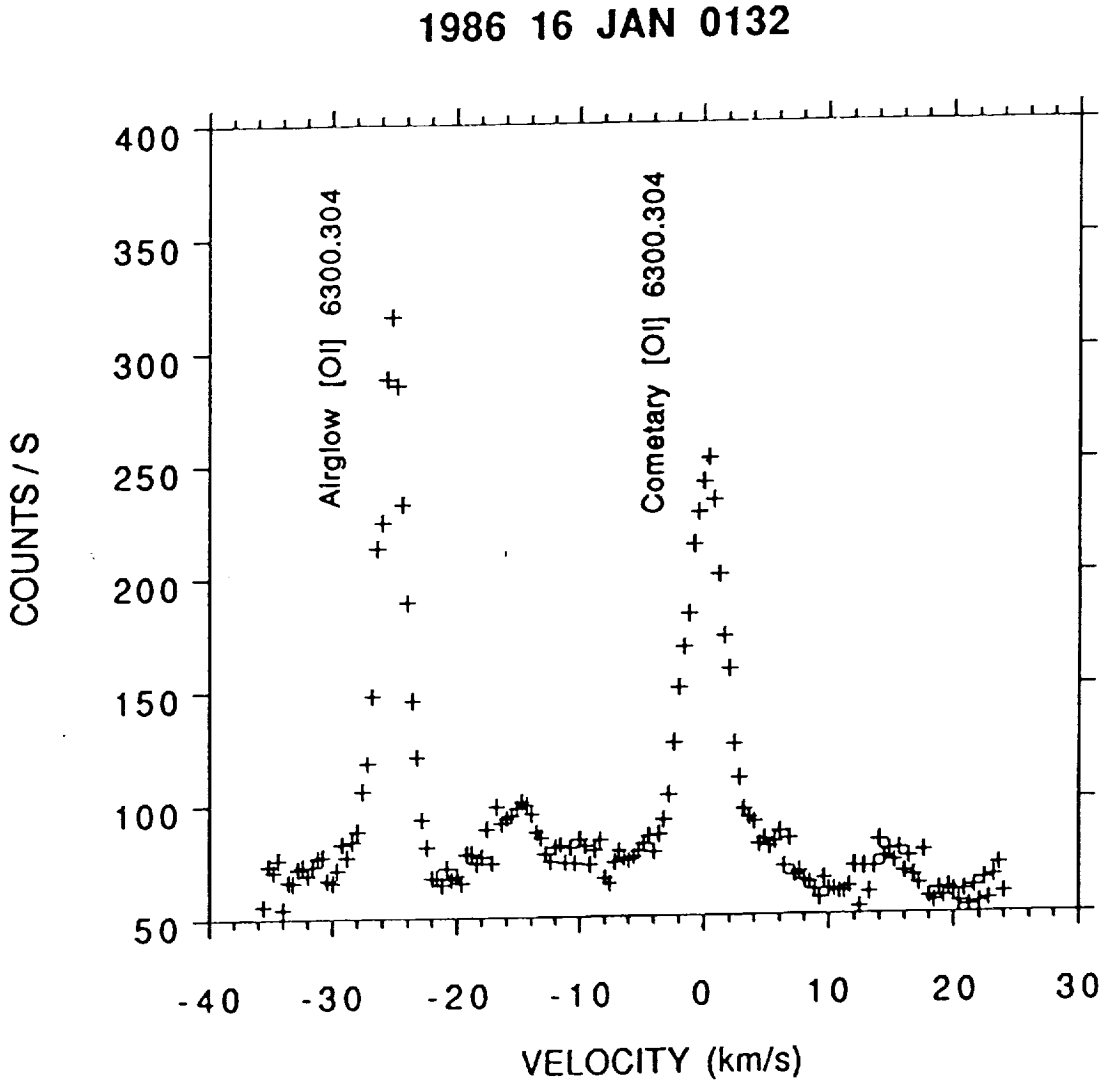
1986 16 JAN 0132
COUNTS / S
400
350
300
250
200
150
100
50
Airglow [OI] 6300.304
Cometary [OI] 6300.304
-40
-30
-20
-10
0
10
20
30
VELOCITY (km/s)

Figure 1

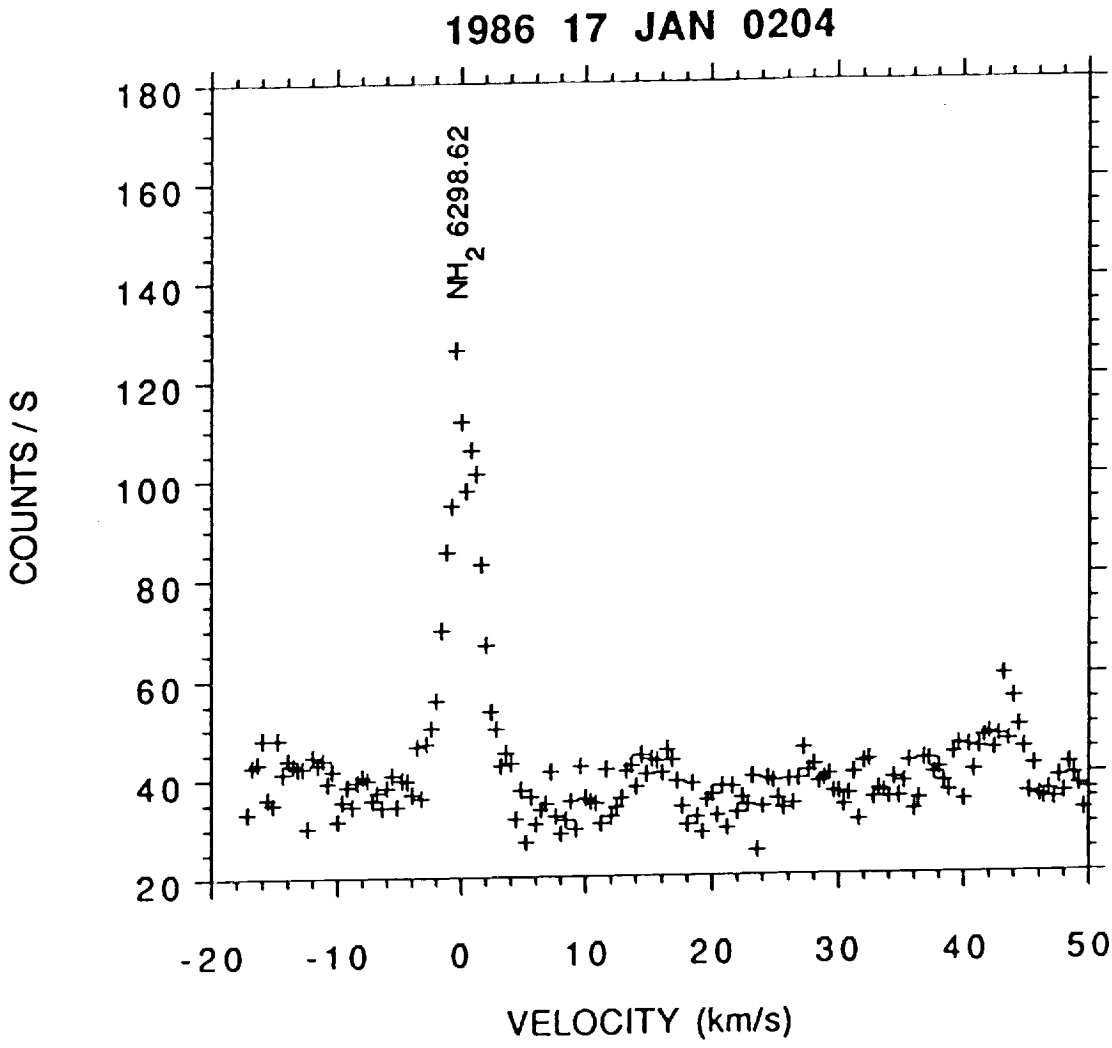
1986 17 JAN 0204
NH_2 6298.62
COUNTS / S
180
160
140
120
100
80
60
40
20
-20
-10
0
10
20
30
40
50
VELOCITY (km/s)

Figure 2

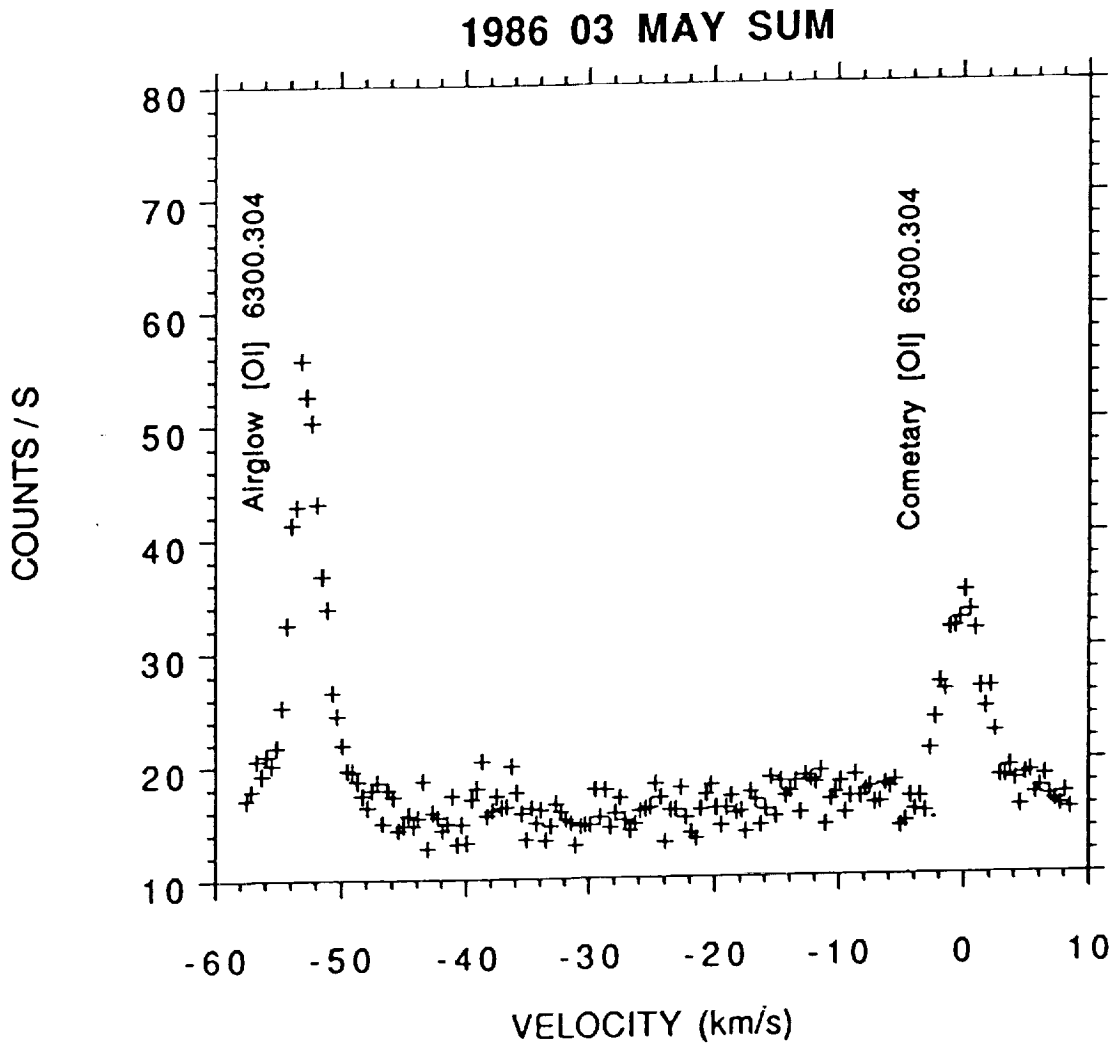
1986 03 MAY SUM
COUNTS / S
80
70
60
50
40
30
20
10
Airglow [OI] 6300.304
Cometary [OI] 6300.304
-60
-50
-40
-30
-20
-10
0
10
VELOCITY (km/s)

Figure 3

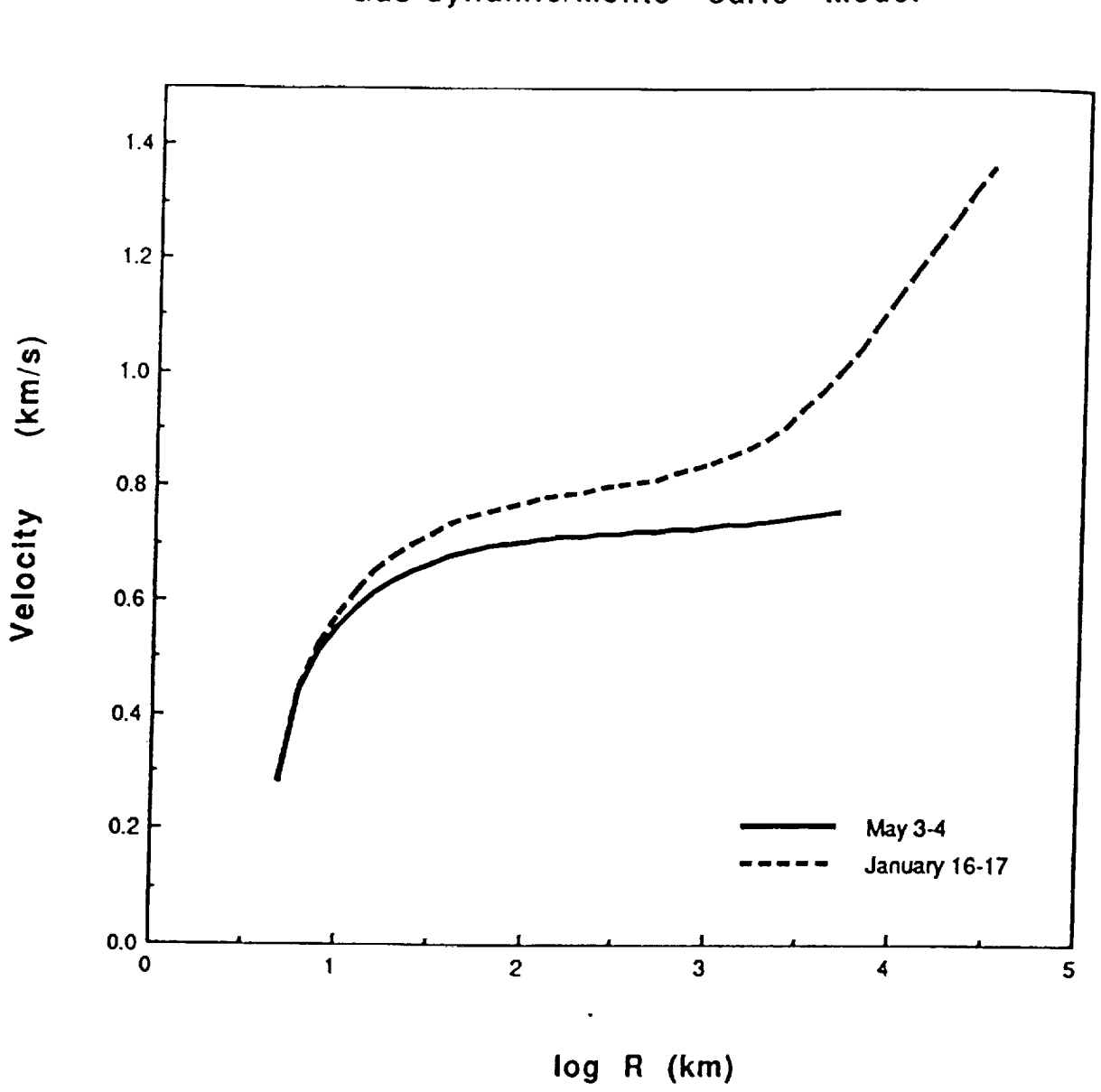
Gas-dynamic/Monte Carlo Model
Velocity (km/s)
1.4
1.2
1.0
0.8
0.6
0.4
0.2
0.0
0
1
2
3
4
5
log R (km)
May 3-4
January 16-17

Figure 4a

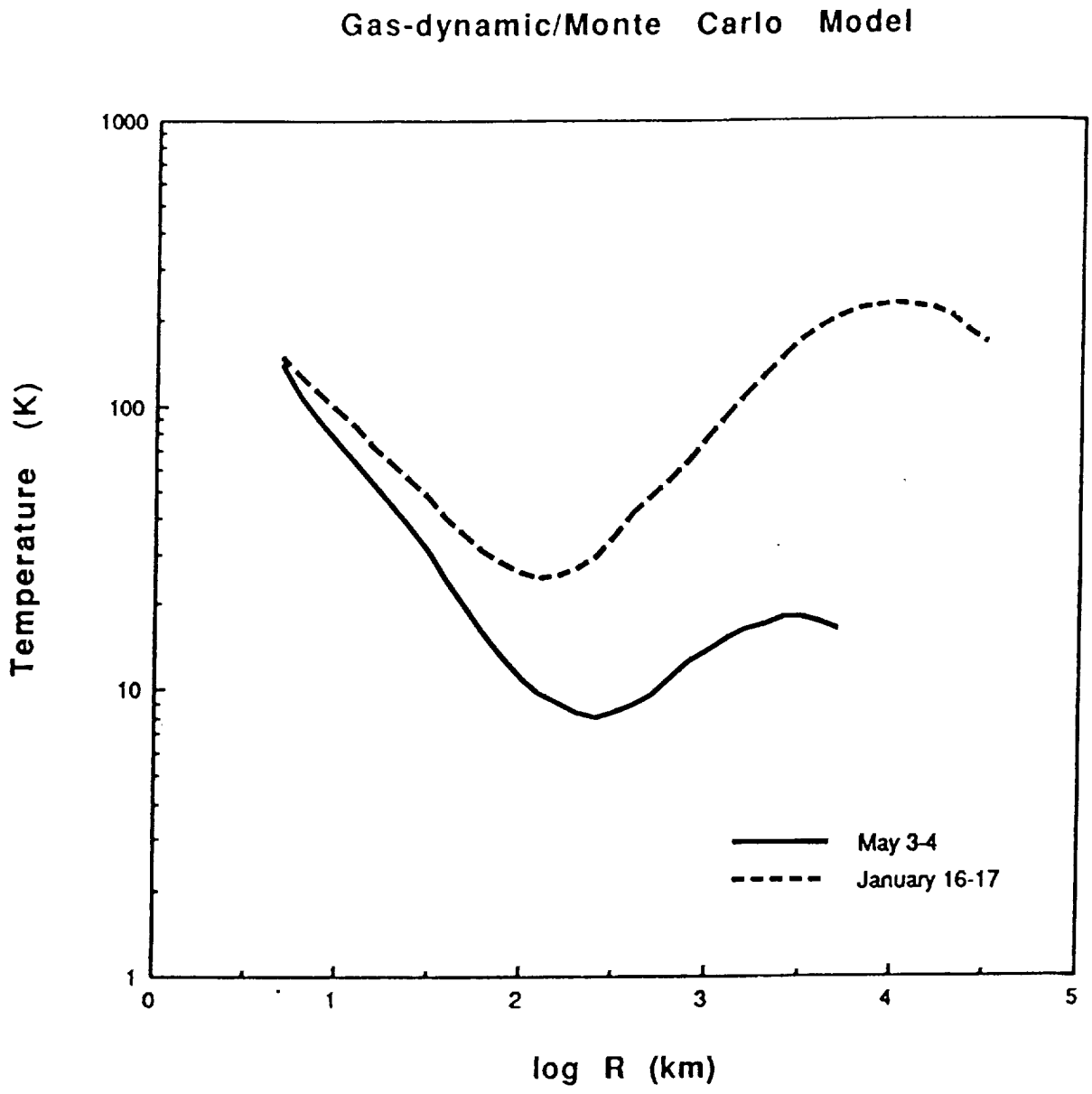
Gas-dynamic/Monte Carlo Model
1000
100
10
1
Temperature (K)
0
1
2
3
4
5
log R (km)
May 3-4
January 16-17

Figure 4b

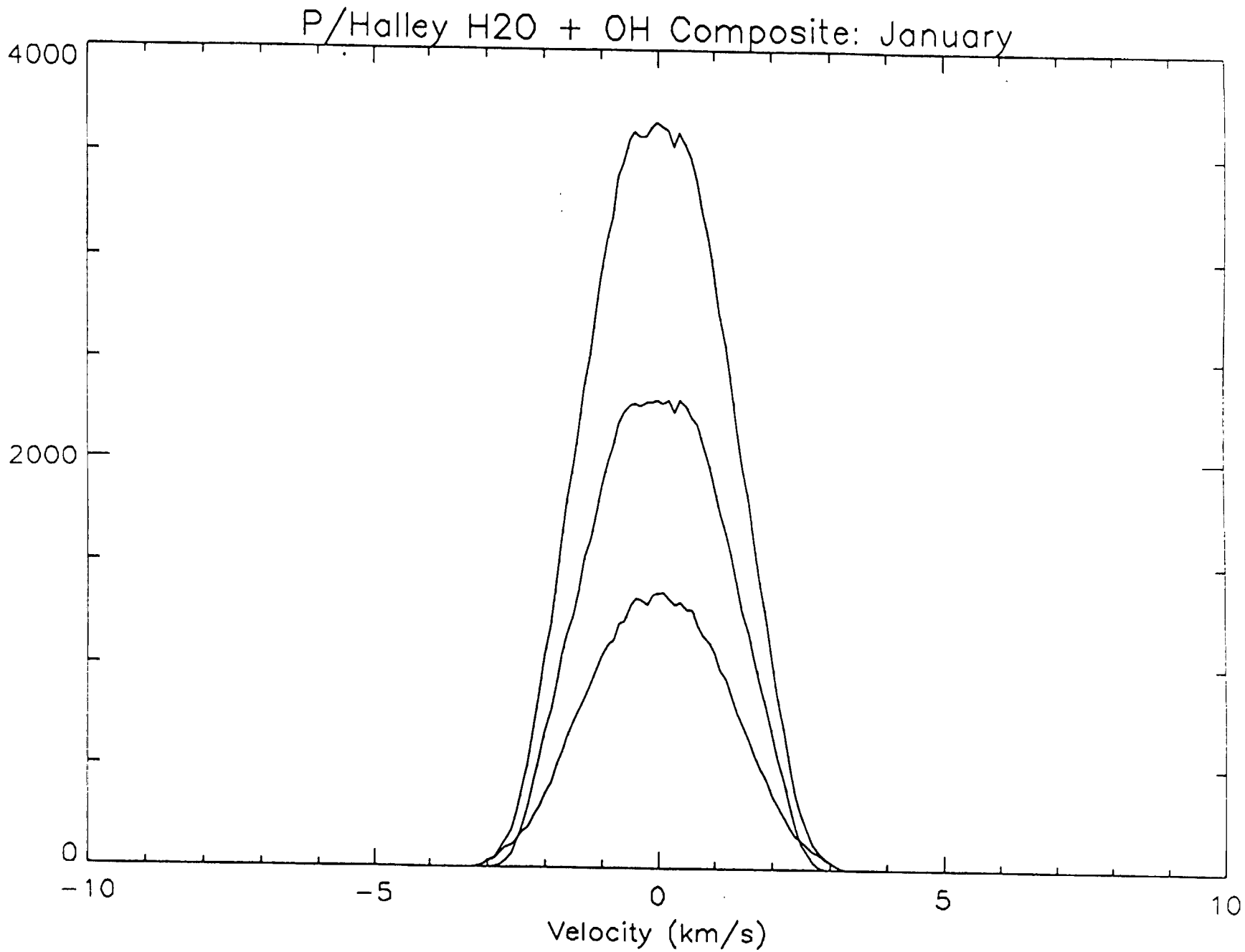
P/Halley H2O + OH Composite: January
4000
2000
0
−10
−5
0
5
10
Velocity (km/s)

Figure 5a

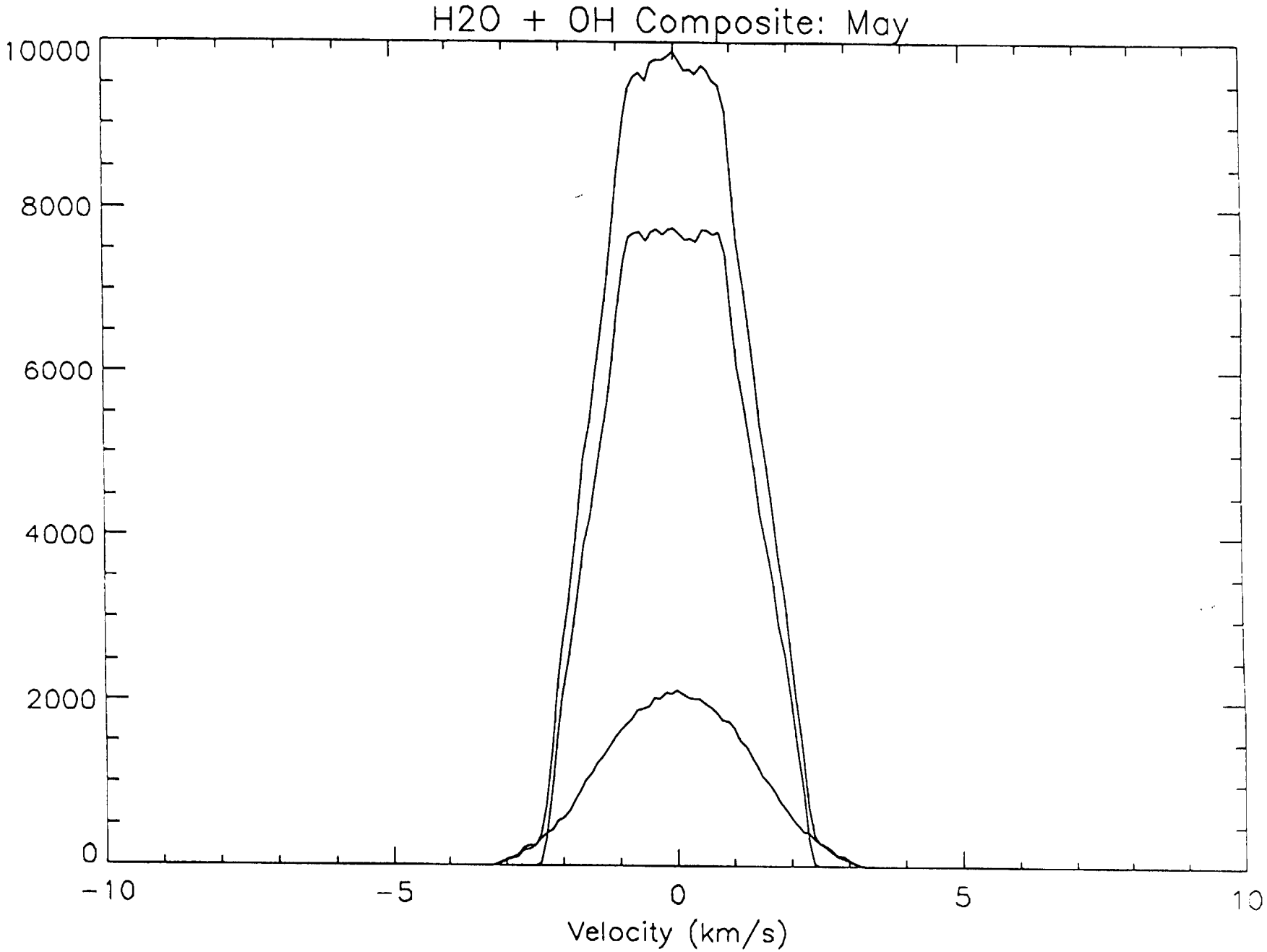
H2O + OH Composite: May
10000
8000
6000
4000
2000
0
-10
-5
0
5
10
Velocity (km/s)

Figure 5b

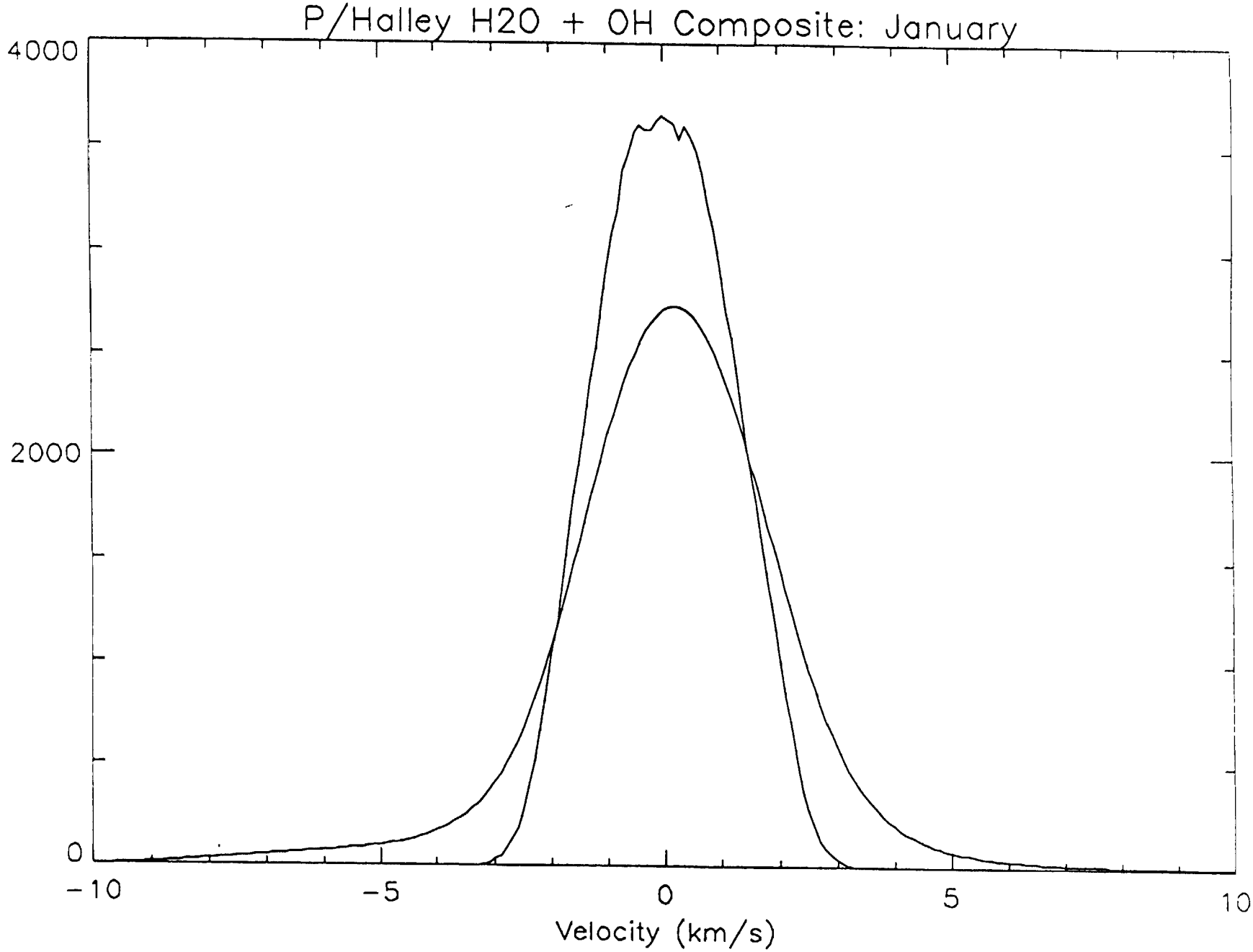
P/Halley H2O + OH Composite: January
4000
2000
0
-10
-5
0
5
10
Velocity (km/s)

Figure 6a

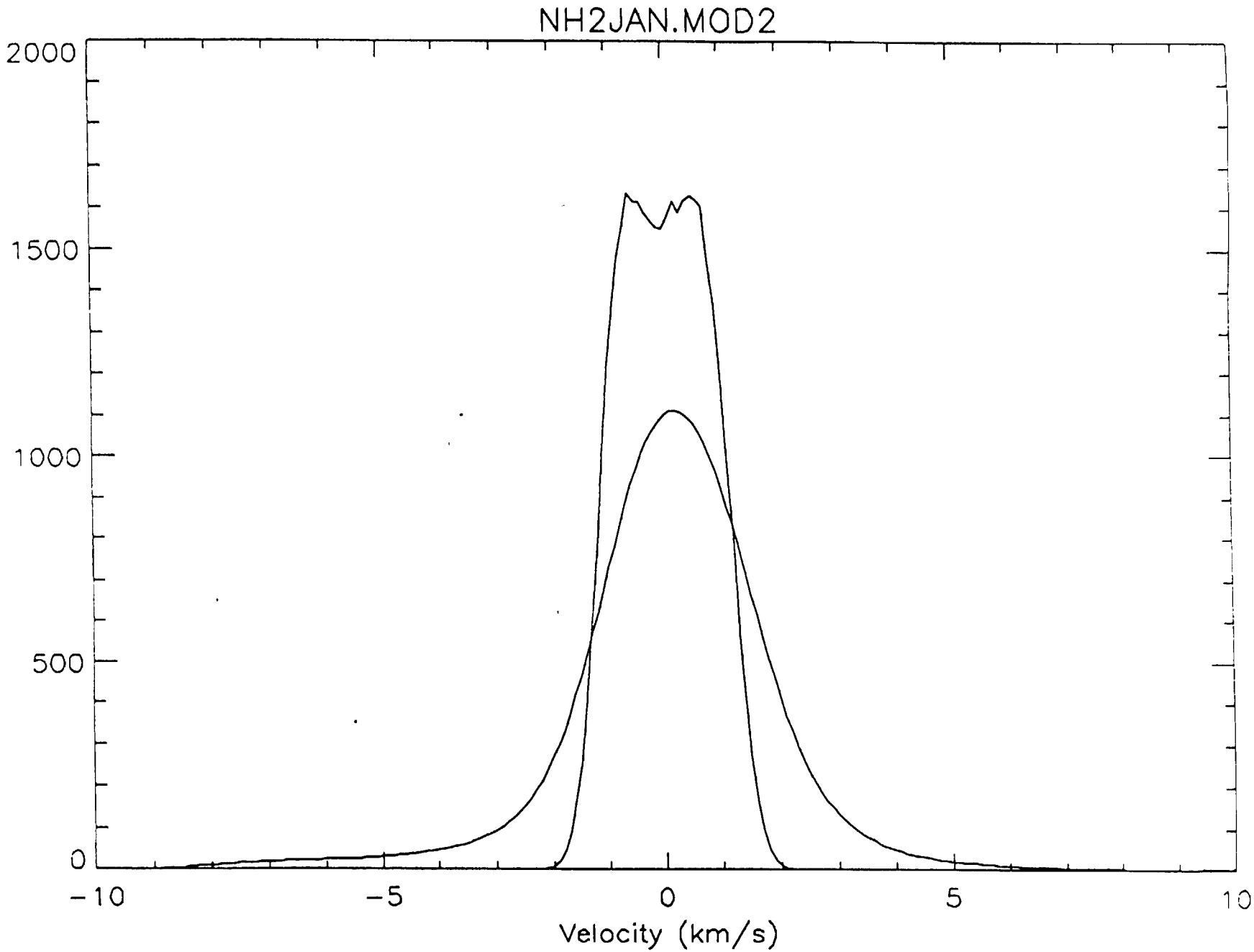

Figure 6b

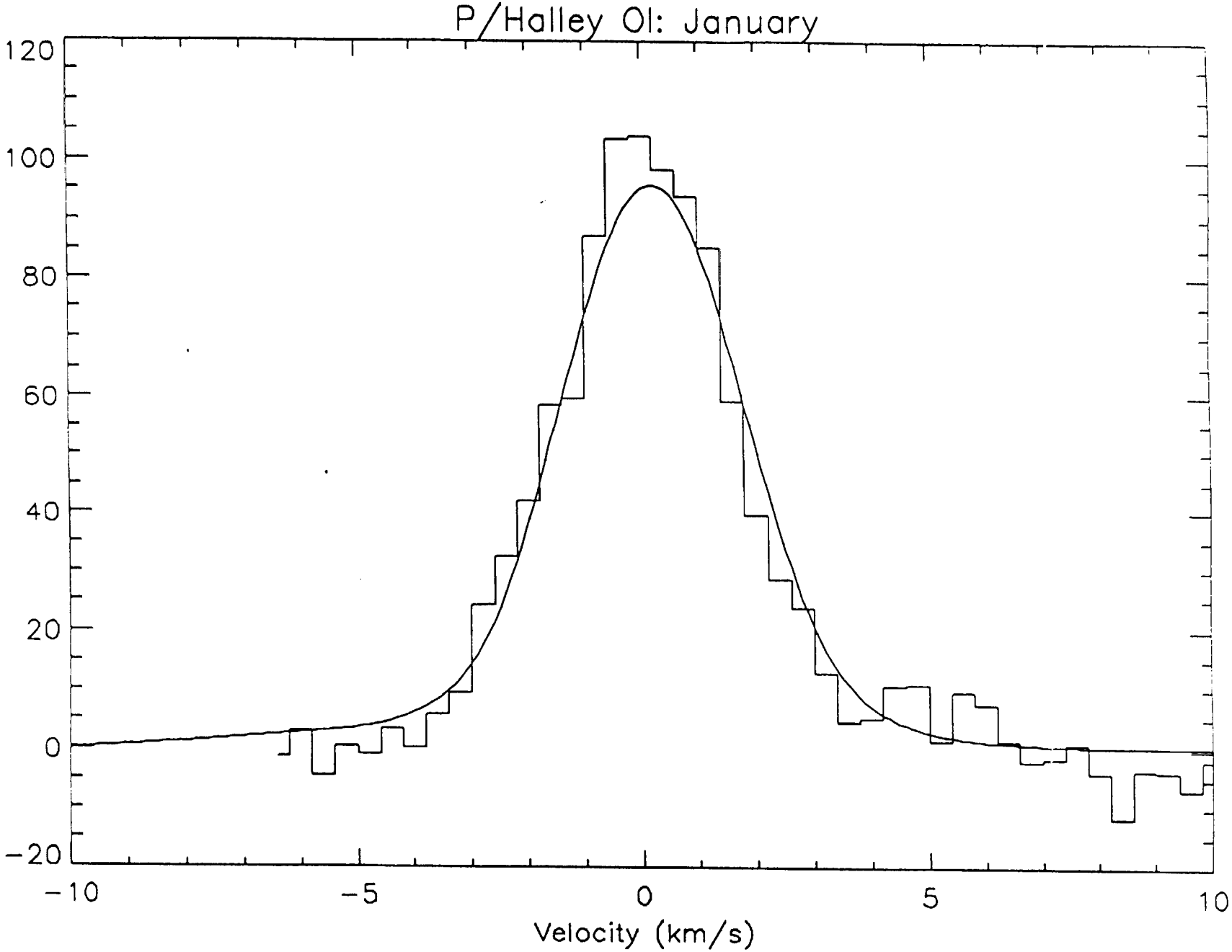
P/Halley OI: January
120
100
80
60
40
20
0
−20
−10
−5
0
5
10
Velocity (km/s)

Figure 7a

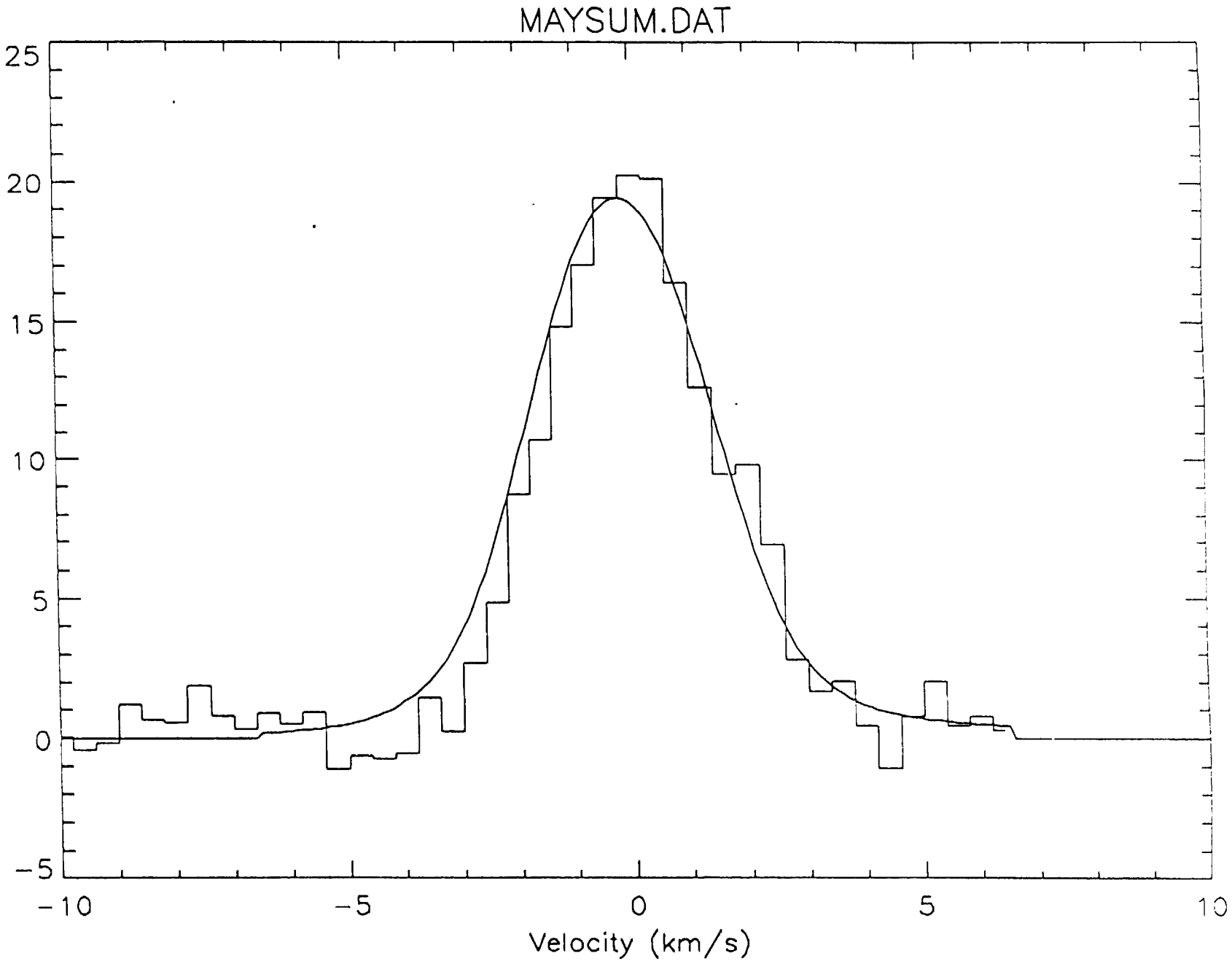

Figure 7b

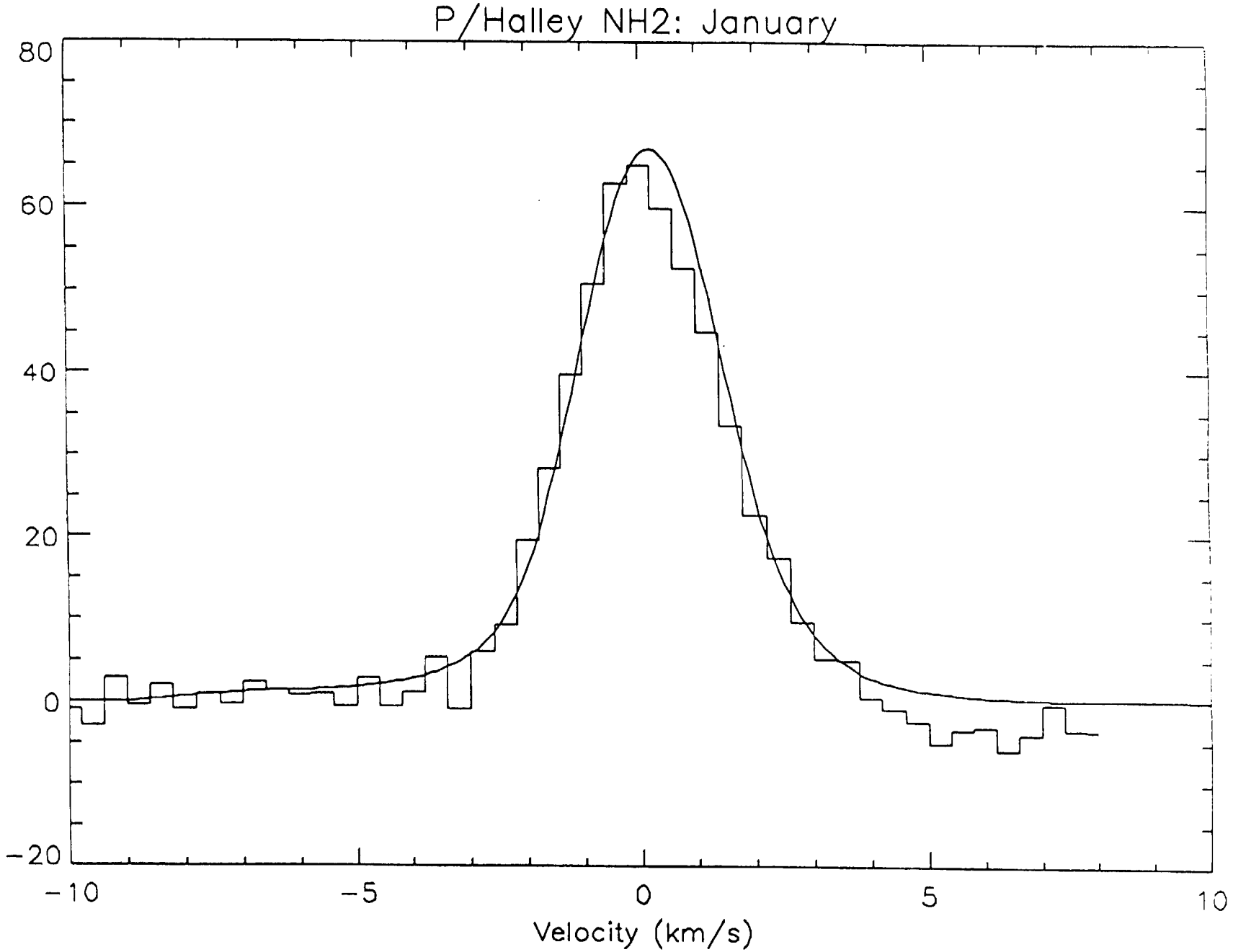

Figure 8

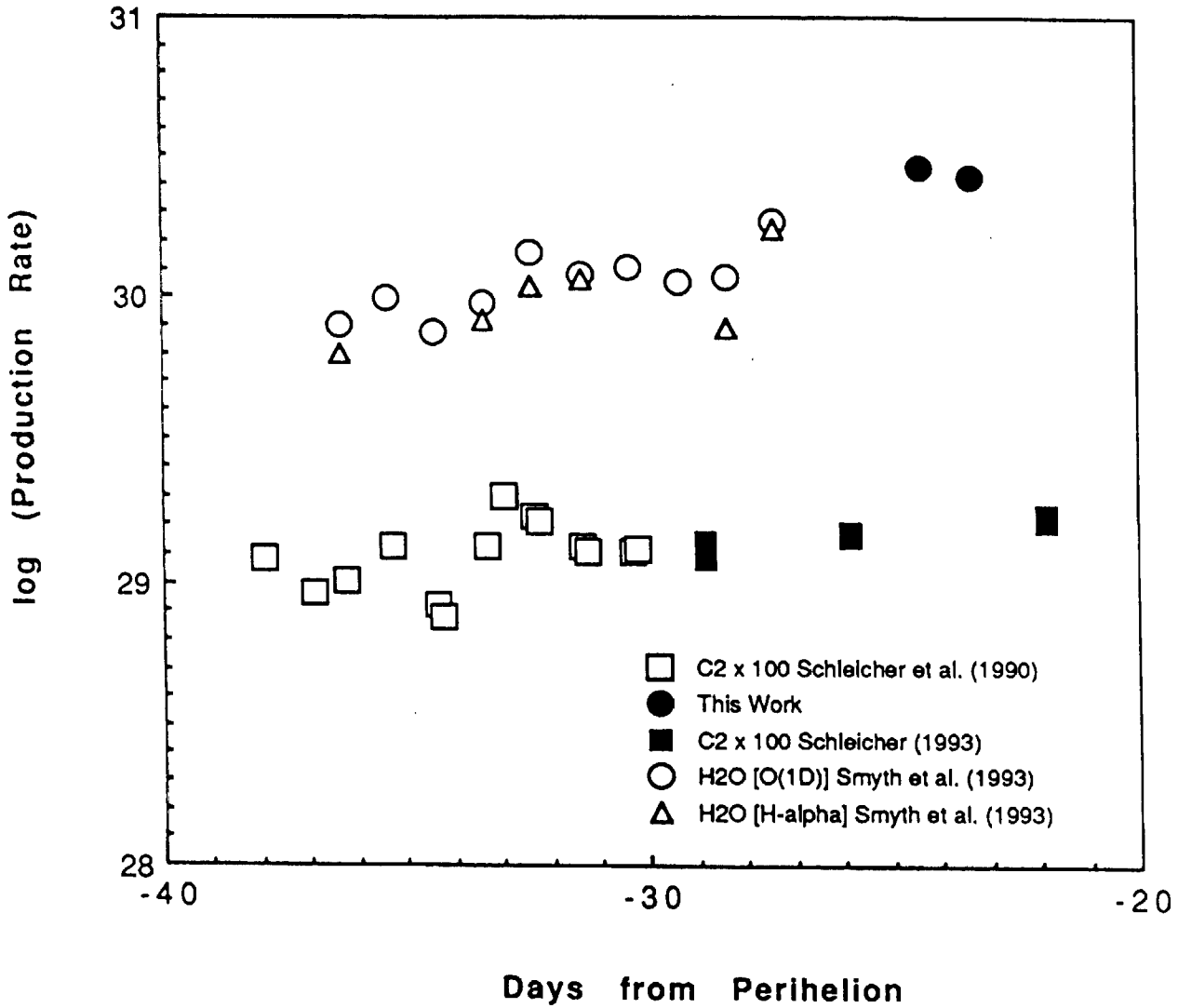
31
30
29
28
-40
-30
-20
log (Production Rate)
Days from Perihelion
C2 x 100 Schleicher et al. (1990)
This Work
C2 x 100 Schleicher (1993)
H2O [O(1D)] Smyth et al. (1993)
H2O [H-alpha] Smyth et al. (1993)

Figure 9

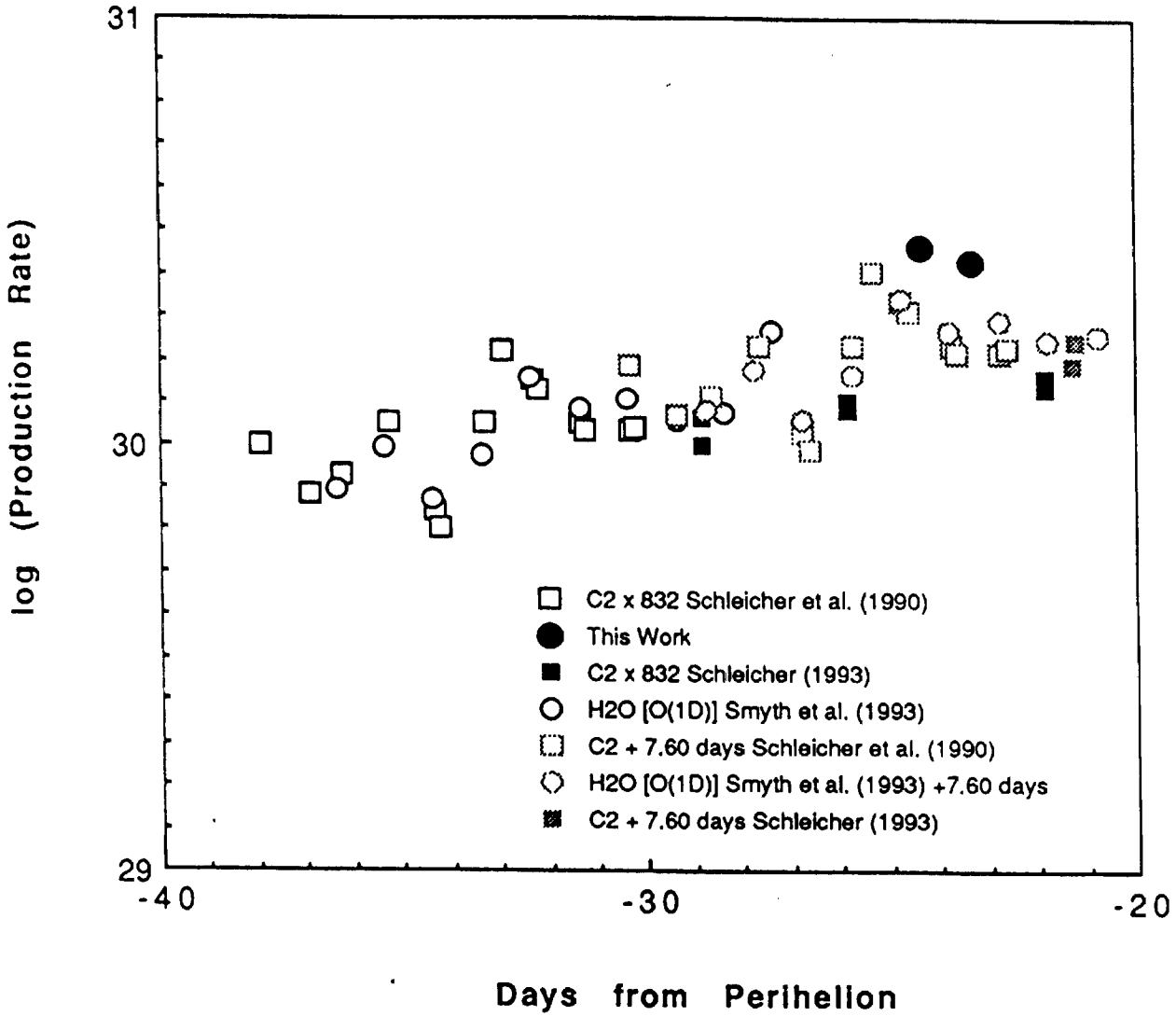
31
30
29
-40
-30
-20
log (Production Rate)
Days from Perihelion
C2 x 832 Schleicher et al. (1990)
This Work
C2 x 832 Schleicher (1993)
H2O [O(1D)] Smyth et al. (1993)
C2 + 7.60 days Schleicher et al. (1990)
H2O [O(1D)] Smyth et al. (1993) +7.60 days
C2 + 7.60 days Schleicher (1993)

Figure 10

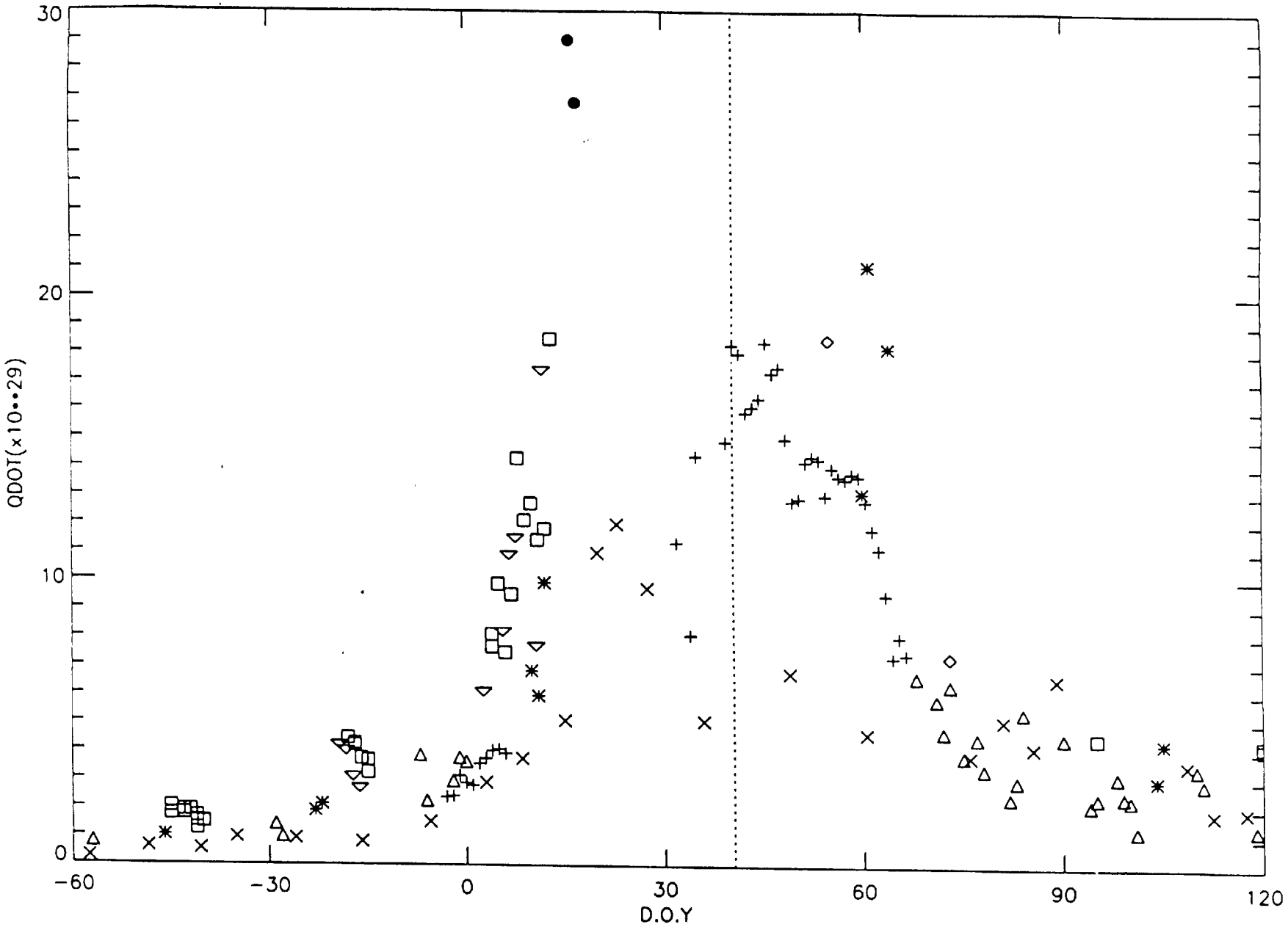

Figure 11